

Adversarial Vulnerability due to On-Manifold Inseparability

Rajdeep Haldar
Purdue University

Yue Xing
Michigan State University

Qifan Song
Purdue University

Guang Lin
Purdue University

Abstract

Recent works have shown theoretically and empirically that redundant data dimensions are a source of adversarial vulnerability. However, the inverse doesn't seem to hold in practice; employing dimension-reduction techniques doesn't exhibit robustness as expected. In this work, we consider classification tasks and characterize the data distribution as a low-dimensional manifold, with high/low variance features defining the on/off manifold direction. We argue that clean training experiences poor convergence in the off-manifold direction caused by the ill-conditioning in widely used first-order optimizers like gradient descent. The poor convergence then acts as a source of adversarial vulnerability when the dataset is inseparable in the on-manifold direction. We provide theoretical results for logistic regression and a 2-layer linear network on the considered data distribution. Furthermore, we advocate using second-order methods that are immune to ill-conditioning and lead to better robustness. We perform experiments and exhibit tremendous robustness improvements in clean training through long training and the employment of second-order methods, corroborating our framework. Additionally, we find the inclusion of batch-norm layers hinders such robustness gains. We attribute this to differing implicit biases between traditional and batch-normalized neural networks.

data distribution exposed during training (Liu et al., 2020). However, they showcase surprising vulnerability to imperceptible perturbations to the input data, hampering the classification performance severely. The perturbed inputs exploiting the vulnerability or attacking the originally trained model are known as *adversarial examples* in the literature (Szegedy et al., 2013; Goodfellow et al., 2014; Madry et al., 2017; Carlini and Wagner, 2017).

In recent years, there has been tremendous progress on the empirical side in developing state-of-the-art attacks and algorithms to defend against adversarial examples; unfortunately, the theoretical foundations explaining the existence of adversarial attacks haven't enjoyed the same pace. Understanding the founding mechanism is critical to developing inherently robust models that naturally align with the human decision-making process and can highlight the fundamental flaws in modern-day model training.

The manifold hypothesis, suggesting that the support of underlying data is a low-dimensional manifold lying in a higher-dimension ambient space, is the most promising theory pertaining to the existence of adversarial examples. Works like Melamed et al. (2024); Haldar et al. (2024) show empirically and theoretically that with a large number of redundant dimensions (e.g., useless background pixels for image tasks), one can generate adversarial examples of arbitrarily small magnitude. In addition, the implicit bias literature (Wei et al., 2019; Lyu and Li, 2019; Lyu et al., 2021; Nacson et al., 2022) suggests clean training leads to a model that is a KKT solution of the *maximum margin problem*. More generally, Rosset et al. (2003) shows that the widely used logistic loss is a *maximizing margin loss*, which extends to deep neural networks.

The notion of a geometrically robust maximum margin classifier is inherited from the theory of Support Vector Machines (SVM). For linear models, the geometric notion of the maximum margin classifier is equivalent to solving the max-margin problem in implicit bias literature. Although the two definitions are not directly comparable for neural networks (non-linear networks), there is an equivalence of sufficiently wide neural net-

1 Introduction

Neural networks exhibit high classification performance and generalize well for test examples drawn from the

works and SVMs or Kernel Machines (KM) in general, accompanied by robustness certificate results (Chen et al., 2021; Domingos, 2020). Based on the equivalence results and visual boundary of neural network classifiers in our experiments (Fig: 3), we expect the max-margin implicit bias of neural networks to enforce robustness and be immune to small magnitude imperceptible attacks. More discussion can be found in the third paragraph of Section 2.

The prior results suggest that a cleanly trained model should exhibit robustness in the absence of redundant dimensions due to its natural inclination toward learning a max-margin classifier. However, in practice, implementing dimension reduction techniques like PCA does not improve model robustness (Alemany and Pissinou, 2020; Aparne et al., 2022). Hence, there is a gap between what we expect and observe.

This work bridges the gap between the theory suggesting robust models in the absence of redundant dimensions and the persistent vulnerability observed in practice. The implicit bias and large margin properties of logistic loss hold at *convergence* to the optimal classifier. We claim that, in practice, convergence isn't attained due to *ill-conditioning* (Goodfellow et al., 2016; Boyd and Vandenberghe, 2004; Nesterov, 2013) when dealing with first-order optimization methods like *gradient-descent*, which adds to the vulnerability of our trained model. Throughout this paper, the default underlying loss for our arguments is the logistic loss or its multivariate counterpart, the cross-entropy loss, as it is the most natural and popular choice of loss for classification problems.

We generalize the idea of off/on-manifold dimensions beyond redundant/useful dimensions as suggested in Haldar et al. (2024); Melamed et al. (2024) to low/high variance features. Even if the data is separable, if it is non-separable in the on-manifold dimensions, the optimal classifier is dependent on the off-manifold dimensions. However, convergence is significantly slower in the off-manifold direction (ill-conditioning), resulting in a suboptimal solution that is not large/maximum margin, leading to adversarial vulnerability.

Figure 1 motivates our framework with an example. Consider a classification problem between birds and insects. Most birds and insects can be distinguished based on wing length (high variance/on-manifold); birds, in general, have much larger wing lengths than insects with small or no wings. However, some insects might have wings larger than the smallest birds, like hummingbirds; hence, we can use the presence of a beak as an additional discrete feature (i.e., low-variance/off-manifold direction) to distinguish them further. Note that the data distribution of birds/insects is separa-

ble using both beak presence and wing length, but it isn't separable solely based on wing length. Figure 2 shows that even though the optimal classifier (attained at convergence) is robust, the estimated decision boundary learned due to lack of convergence in the off-manifold direction is not robust. This is caused by the ill-conditioned nature of the training, which is related to the extent of low-dimensionality, which is characterized by the ratio of on/off-manifold variances.

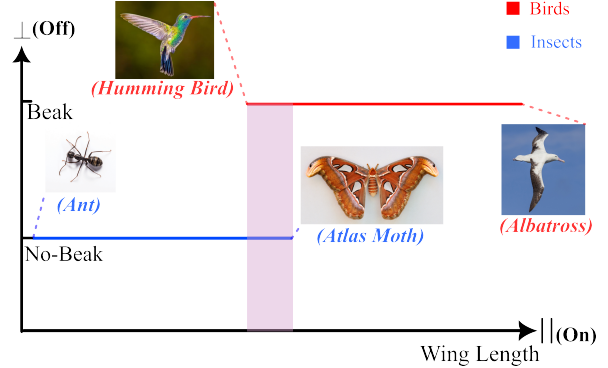


Figure 1: Binary classification between birds and insects. The purple region represents overlap in the on-manifold feature, where only the off-manifold feature can distinguish between the two classes.

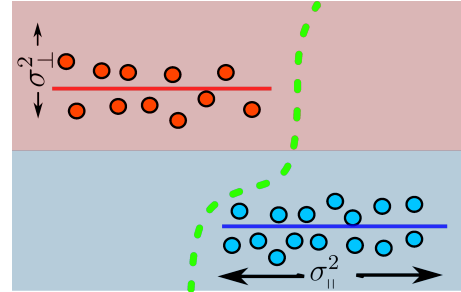


Figure 2: Optimal classifier robustly separates the ambient space into red and blue regions. The estimated decision boundary (green) is suboptimal and vulnerable even though it separates the data manifold accurately.

To further illustrate the crucial concepts of on/off manifold and low-dimensionality, we give two mathematical examples below

Example 1. $x_1 \sim N(0, \sigma_{||}^2), x_2 \sim N(0, \sigma_{\perp}^2)$ be distribution of two features, as $\sigma_{||} \approx \sigma_{\perp}$ the data resembles a 2-D disk. However, as $\sigma_{\perp}/\sigma_{||} \rightarrow 0$, the distribution converges to a 1-D line. The one-dimensional direction is dictated solely by the high-variance feature x_1 or the on-manifold feature.

Example 2. Consider a 3-D sphere described in polar coordinates (R, ϕ, ψ) . As $\sigma_R \ll \sigma_{\phi} \simeq \sigma_{\psi}$ the data distribution resembles a 2-D shell, with on-manifold direction dictated by the two angles ψ, ϕ and off-manifold

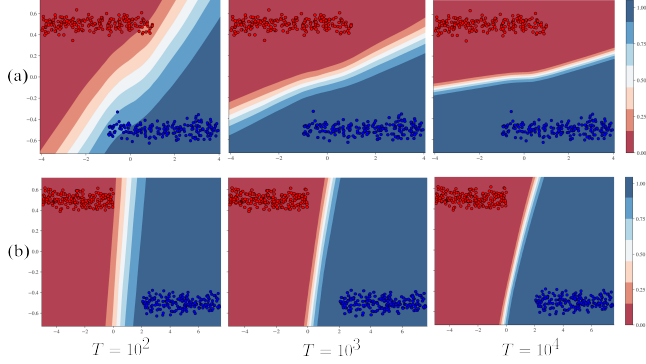


Figure 3: Neural Network estimated decision boundary for T training epochs. Training and testing accuracy is 100% for all $T \geq 10^2$. Data distribution is on-manifold (a) inseparable (b) separable.

being R direction. Similarly, if both $\sigma_R, \sigma_\phi \ll \sigma_\psi$, then the sphere becomes a 1-D circle, with on-manifold direction dictated only by ψ . The ratio of the high-variance/low variance determines the extent of dimensionality.

We summarize our key contributions as the following informal theorems:

Theorem 1.1 (Informal version of Theorem 4.2). *Convergence to the optimal parameter is faster and independent of dimensionality in the on-manifold direction compared to the off-manifold direction. Furthermore, as dimensionality reduces, the convergence rate for the off-manifold direction worsens.*

Theorem 1.2 (Informal version of Theorem 4.3). *There is an error threshold, determined by the separability in the on-manifold direction, which can be quickly reached, but reducing error below that threshold is slower and depends on data dimensionality.*

When data is inseparable in on-manifold direction, Figure 3(a) illustrates the improvement in shape and robustness of the decision boundary over time due to slow convergence in the off-manifold direction. Figure 3(b) shows when data is on-manifold separable, the shape of the optimal decision boundary solely depends on the on-manifold direction and is stable due to fast convergence.

It is known that second-order optimization methods like Newton’s method are immune to ill-conditioning. Therefore, we promote using second-order methods (Section 5) to guarantee fast convergence and, in turn, enjoy robustness gains in cleanly trained models. We conduct experiments to support our claim (Section 6).

2 Related Works

Adversarial Vulnerability Explained via Manifold Hypothesis: Stutz et al. (2019) introduced the distinction between *on/off-manifold adversarial examples* and their role in robustness and generalization. Shamir et al. (2021) showed empirically that clean-trained classifiers align with a low dimensional *dimple-manifold* around the data, making them vulnerable to imperceptible perturbations. Zhang et al. (2022) decomposed the adversarial risk into geometric components motivated by manifold structure. Haldar et al. (2024); Melamed et al. (2024) theoretically establish a relationship between the *dimension gap* (induced by low-dimension data manifold) and adversarial vulnerability.

Attack/Defense systems based on manifold hypothesis: Xiao et al. (2022) uses a generative model to learn manifold and create on-manifold attacks. Jha et al. (2018); Lindqvist et al. (2018); Lin et al. (2020) have tried to learn the underlying manifold to detect and defend adversarial examples outside the data manifold.

To the best of our knowledge, our work is the first: Extending the notion of on/off manifold dimensions in terms of feature variances rather than utility; Drawing connections between on-manifold separability, ill-conditioning, and adversarial vulnerability.

Implicit Bias and Robustness Frei et al. (2024) show that max-margin implicit bias of neural networks aren’t the most robust model. However, the order of attack strength in this work is comparable to the signal strength, and reduces to natural/on-manifold attack scenario mentioned in Haldar et al. (2024). These attacks are perceptible by humans and relatively large magnitude. We still expect a natural robustness to imperceptible attacks or small magnitude attacks in absence of redundant dimension, based on prior discussion. Min and Vidal (2024) shows that under poly-ReLU activation implicit bias can be robust to larger attacks.

3 Problem Setup

This section describes the technical setting and assumptions used for our main results in section 4.2.

3.1 Notation

Throughout this paper, we will use the subscripts \parallel, \perp to denote mathematical objects corresponding to on-manifold and off-manifold, respectively. The notation $\mathbf{1}_d$ denotes the concatenated vector of ones of length d .

For any two vectors u, v such that $u_i \leq v_i \forall i$, we can define a hypercube $[u, v]$ such that if $z \in [u, v]$ then for each i , $z_i \in [u_i, v_i]$. Denote \mathbf{I}_d as the identity matrix of d dimensions. Notation $\Omega(\cdot)$ is the usual asymptotic lower bound notation. For $a, b \in \mathbb{R}$, $a \preceq b \iff a \leq b \cdot c$ for some $c > 0$. Note that the notation \preceq also works for negative sequences a and b (i.e., $a \preceq b$ implies $|b| \preceq |a|$ when a and b are negative). Denote \odot as the Hadamard product.

3.2 Assumption on Data Distribution

We denote the underlying signal of the data with $x \in \mathbb{R}^D$ and its corresponding label as $y \in \{-1, +1\}$. We study a binary classification problem with the data pair (x, y) .

Our signal can be decomposed as $x = (x_{\parallel}, x_{\perp})$, where $x_{\parallel} \in \mathbb{R}^d$ and $x_{\perp} \in \mathbb{R}^g$ are the on/off manifold components respectively. Corresponding to each class, define d -dimensional hypercubes of side l as $\mathcal{I}_{\parallel}^{(-1)} = [-(l-k) \cdot \mathbf{1}_d, k \cdot \mathbf{1}_d]$ and $\mathcal{I}_{\parallel}^{(+1)} = [-k \cdot \mathbf{1}_d, (l-k) \cdot \mathbf{1}_d]$. The parameter k controls the overlap between the two hypercubes in the on-manifold direction. We assume that conditioned on the label the on-manifold signal is uniformly drawn from such hyper-cubes $x_{\parallel}|y \sim \mathcal{U}(\mathcal{I}_{\parallel}^{(y)})$ with means $\mu_{\parallel}^{(y)} = \frac{y(l-2k)}{2} \cdot \mathbf{1}_d$ and covariance $\sigma_{\parallel}^2 \cdot \mathbf{I}_d = \frac{l^2}{12} \cdot \mathbf{I}_d$ respectively. Similarly, define non-overlapping symmetric hyper-cubes $\mathcal{I}_{\perp}^{(y)} = [\mu_{\perp}^{(y)} - \sqrt{3}\sigma_{\perp} \cdot \mathbf{1}_g, \mu_{\perp}^{(y)} + \sqrt{3}\sigma_{\perp} \cdot \mathbf{1}_g]$ such that $\mathcal{I}_{\perp}^{(-1)} \cap \mathcal{I}_{\perp}^{(+1)} = \emptyset$, and $x_{\perp}|y \sim \mathcal{U}(\mathcal{I}_{\perp}^{(y)})$ with means $\mu_{\perp}^{(y)}$ and covariance $\sigma_{\perp}^2 \cdot \mathbf{I}_g$. The class probabilities themselves are binomial with probability π i.e. $P(y = 1) = \pi$ and $P(y = -1) = 1 - \pi$. Also, $\|\mu_{\perp}^{(y)}\| < \infty$ and $\sigma_{\perp}/\sigma_{\parallel} < 1$.

To explain the above assumption, the data is essentially uniformly distributed over two high-dimensional rectangles corresponding to each class. Due to the non-overlapping off-manifold distributions, the two rectangles are linearly separable in the ambient D -dimensional space. However, there is an overlap in the on-manifold distribution controlled by k . The x and x_{\perp} distributions are linearly separable, but x_{\parallel} is not for $k \neq 0$. The ratio of the variances $\sigma_{\perp}^2/\sigma_{\parallel}^2 < 1$ characterizes the low-dimensional manifold structure. Our data model is a mathematical representation of Figures 2, 3.

Overlapping coefficient In order to formulate the extent of non-separability in the on-manifold distribution we borrow the concept of *overlapping coefficient* (OVL) from traditional statistics. For any two probability densities $f_1(x), f_2(x)$ the overlapping coefficient is defined as $\nu = \int_{\mathcal{D}} \min(f_1(x), f_2(x)) dx$ where \mathcal{D} is the support. Note that $\nu \in [0, 1]$, and essentially represents the probability of x being drawn from the minority distribution. In the context of a naive

Bayes classifier, ν represents the probability of misclassification or area of conflict. We can quantify non-separability for the on-manifold distribution by computing $\nu = \int \min(\mathcal{U}(\mathcal{I}_{\parallel}^{(-1)}), \mathcal{U}(\mathcal{I}_{\parallel}^{(+1)})) dx = (k/l)^d$. As k increases, geometrically, our on-manifold hypercubes overlap more, which is consistent with ν . Later, we will see how the non-separability of the on-manifold component affects our classifier learning.

3.3 Models

For our binary classification problem, we work with the logistic loss $\ell(z) = \ln(1 + e^{-z})$. We will denote $f(x, \gamma)$ with real output as the score predicted by our classifier for a particular data point x and parameter vector γ . The expected loss of the classifier over the data distribution is $\mathcal{L}(\gamma) = \mathbb{E}_{x,y} \ell(y \cdot f(x, \gamma))$. The clean training is the optimization problem $\min_{\gamma \in \Gamma} \mathcal{L}(\gamma)$ where Γ is a compact parameter space. Let $\gamma^* = \arg \min_{\gamma \in \Gamma} \mathcal{L}(\gamma)$, then working with compact space ensures $\|\gamma^*\|$ is finite and makes analysis tractable. This work considers the linear model and the two-layer linear network.

3.3.1 Logistic Regression

In the linear setup, $\gamma = \theta$ where $\theta \in \mathbb{R}^D$ is the coefficient vector of logistic regression, $f(x, \theta) = \theta^T x$. We implement a first-order gradient descent optimization scheme with step size α to obtain the minimizer in this scenario. The t^{th} iteration step is as follows:

$$\theta^{(t+1)} = \theta^{(t)} - \alpha \nabla_{\theta} \mathcal{L}(\theta^{(t)}) \quad (1)$$

Parameter components Corresponding to x_{\parallel}, x_{\perp} we have $\theta_{\parallel}, \theta_{\perp}$ such that $\theta^T x = \theta_{\parallel}^T x_{\parallel} + \theta_{\perp}^T x_{\perp}$. Naturally, the notion of on/off manifold components translates to $\theta = (\theta_{\parallel}, \theta_{\perp})$.

3.3.2 Two Layer linear network

For the linear network, we over-parametrize the logistic regression case with $\theta = \mathbf{A}^T w$, where $\mathbf{A} \in \mathbb{R}^{m \times D}$ is a matrix representing the weights of the first layer with m -neurons, and $w \in \mathbb{R}^m$ represents the weights of the output layer. $\gamma = (\text{vec } \mathbf{A}, w)$ and the model is $f(x, \gamma) = w^T \mathbf{A} x$. The parameter space is the product space $\Gamma = \mathcal{A} \times \mathcal{W}$ of the first and second layers. As we are working with compact spaces, minimization over the product space is equivalent to sequential minimization over the first and second layer, i.e.

$$\min_{\gamma \in \mathcal{A} \times \mathcal{W}} \mathcal{L}(\gamma) = \min_{w \in \mathcal{W}} \min_{\text{vec } \mathbf{A} \in \mathcal{A}} \mathcal{L}(\gamma)$$

Consequently, we can implement an alternating gradient descent (AGD) algorithm with step sizes α_1, α_2 to

obtain the minimizer. The t^{th} step of AGD involves the following two gradient descent steps:

$$w\text{-step: } w^{(t+1)} = w^{(t)} - \alpha_1 \nabla_w \mathcal{L}(w^{(t)}, \mathbf{A}^{(t)}) \quad (2)$$

$$\mathbf{A}\text{-step: } \mathbf{A}^{(t+1)} = \mathbf{A}^{(t)} - \alpha_2 \nabla_{\mathbf{A}} \mathcal{L}(w^{(t+1)}, \mathbf{A}^{(t)}) \quad (3)$$

Identifiability issue For the two-layer model, the optimal parameter $\gamma^* = (\text{vec } \mathbf{A}^*, w^*)$ isn't unique, however the corresponding logistic regression coefficient $\theta^* = \mathbf{A}^{*T} w^*$ is unique and identifiable. The AGD steps in equations (2, 3) induce a sequence in θ as well, with $\theta^{(2t)} = \mathbf{A}^{(t)T} w^{(t)}$ and $\theta^{(2t+1)} = \mathbf{A}^{(t)T} w^{(t+1)}$. In the subsequent section, we can use this identification to tackle convergence rates of AGD in terms of θ and the loss $\mathcal{L}(\theta) = \mathcal{L}(w, \mathbf{A})$. Furthermore, the notion of on/off manifold parameters can be extended in the two-layer settings in terms of $\theta = \mathbf{A}^T w = (\theta_{\parallel}, \theta_{\perp})$.

Orthogonalization For technical simplicity, we consider an orthogonalization step in addition to the w and \mathbf{A} -steps. That is, before the t^{th} iteration, $\mathbf{A}^{(t)}$ is column-orthogonalized such that $\mathbf{A}^{(t)T} \mathbf{A}^{(t)} = \mathbf{I}_D$, and $w^{(t)}$ is recalibrated to preserve $\theta^{(t)}$, i.e., $\mathbf{A}^{(t)T} w^{(t)}$ keeps the same after orthogonalization. However, this assumption is practical, as orthogonality improves generalizability and curbs vanishing gradient issues. (Li et al., 2019; Achour et al., 2022)

4 Main Results

4.1 Motivation

Consider the expected gradient and hessian of the loss w.r.t. the identifiable parameter θ . Denote the score as $z = f(x, \gamma)$ and $\sigma(v) = (1 + \exp(-v))^{-1}$ as the standard sigmoid function.

$$\nabla_{\theta} \mathcal{L}(\gamma) = - \mathbb{E}_{x, y} y x \sigma(-y \cdot z) \quad (4)$$

$$\nabla_{\theta}^2 \mathcal{L}(\gamma) = \mathbb{E}_{x, y} x x^T \sigma(z) \sigma(-z) \quad (5)$$

Eq. (4) is the gradient over the distribution over x . Thus, for x_{\parallel} belonging to the well-separated region, the gradients are accumulated constructively; in contrast, for all x_{\parallel} belonging to the overlapping region, gradients from each class cancel out and accumulate destructively. This implies that as the overlapping or ν increases, we expect weaker gradients for learning \parallel direction. Furthermore, Eq. (5) showcases the hessian/curvature of the loss w.r.t. θ . Notice that the curvature is implicitly dependent on the term $\mathbb{E} x x^T$, which essentially captures the covariance structure of the data. The variance in the \parallel direction is controlled by σ_{\parallel}^2 inducing a larger curvature, compared to the variance in the \perp

direction inducing a small or flatter curvature. When implementing first-order gradient methods, the step size is bounded by the inverse of the largest curvature σ_{\parallel}^{-2} ; As we want to change the parameters carefully, if the loss is sensitive in certain directions. However, this leads to slower learning in the flatter region, in this case, \perp direction. Consequently, we expect faster convergence in the \parallel direction and slower convergence in the \perp direction, leading to a suboptimal solution with poor margins that is vulnerable to adversarial examples.

Technically, at a very high level, we bound the loss hessian based on variance matrices derived from the data structure. Subsequently, we use Taylor expansions of the loss, Lipschitz smoothness, strong convexity and PL-inequality-based arguments to derive parameter/loss convergence rates.

We formalize the prior intuitions in the following subsection with our main theorems.

4.2 Theorems

For both the logistic regression and two-layer linear network case, we denote the change in loss from $\theta^t \rightarrow \theta^{t+1}$ as: $\Delta \mathcal{L}(t) = \mathcal{L}(\theta^{(t+1)}) - \mathcal{L}(\theta^{(t)})$. Furthermore, the change in loss contributed by the on/off manifold direction is denoted by $\Delta_{\parallel} \mathcal{L}(t) = \mathcal{L}(\theta_{\parallel}^{(t+1)}, \theta_{\perp}^{(t)}) - \mathcal{L}(\theta^{(t)})$ and $\Delta_{\perp} \mathcal{L}(t) = \mathcal{L}(\theta_{\parallel}^{(t)}, \theta_{\perp}^{(t+1)}) - \mathcal{L}(\theta^{(t)})$ respectively.

Theorem 4.1 (Progressive bounds). *Given (x, y) follows data distribution described in Section 3.2. For the t^{th} iterate of θ induced by GD (Eq. (1)), w -step (Eq. (2)) or \mathbf{A} -step of AGD (Eq. (3)) we have:*

$$\begin{aligned} \nabla_{\theta_{\parallel}} \mathcal{L}(\theta^{(t)}) &= -(1 - \nu) \vec{c}_1 \odot \mathbb{1}_d \cdot l^{-k/2} + \nu \vec{c}_2 \odot \mathbb{1}_d \cdot k/2 \\ \nabla_{\theta_{\perp}} \mathcal{L}(\theta^{(t)}) &= -\pi(\vec{c}_3 \odot \mu_{\perp}^{(1)}) + (1 - \pi)((\mathbb{1}_g - \vec{c}_6) \odot \mu_{\perp}^{(-1)}) \\ &\quad - (\vec{c}_4 + \vec{c}_5) \odot \mathbb{1}_g \cdot \sigma_{\perp}/4 \end{aligned}$$

Furthermore, for appropriate choice of step sizes $\alpha, \alpha_1, \alpha_2 \preceq \sigma_{\parallel}^{-2}$, we have:

$$\Delta_{\parallel} \mathcal{L}(t) \preceq -\|\nabla_{\theta_{\parallel}} \mathcal{L}(\theta^{(t)})\|^2 \cdot \sigma_{\parallel}^{-2}; \quad (6)$$

$$\Delta_{\perp} \mathcal{L}(t) \preceq -\|\nabla_{\theta_{\perp}} \mathcal{L}(\theta^{(t)})\|^2 \cdot \sigma_{\parallel}^{-2}$$

$$\Delta \mathcal{L}(t) \preceq -\|\nabla_{\theta} \mathcal{L}(\theta^{(t)})\|^2 \cdot \sigma_{\parallel}^{-2} \quad (7)$$

Where \vec{c}_i are vectors dependent on t with all their elements positive and < 1 ;

As gradient norms and the variances are positive, Eq. (6) and Eq. (7) imply that at each step of GD or AGD, the overall loss strictly decreases. In particular, the loss improves strictly in both \perp, \parallel directions.

Effect of ν Eq. (4.1) decomposes the gradient in the on-manifold direction into two components corresponding to the well-separated and overlapping regions of the on-manifold distribution, respectively. Notice

that the two terms are competing with each other, and as ν (overlapping coefficient) initially increases, $\|\nabla_{\theta_{\parallel}} \mathcal{L}(\theta^{(t)})\|$ tends to decrease due to cancellation. Hence, the loss improvement in \parallel direction also diminishes (Eq. (6)). With the extreme increase in ν even if $\|\nabla_{\theta_{\parallel}} \mathcal{L}(\theta^{(t)})\|$ is large, the classifier becomes agnostic of the original class direction, due to shift in the gradient direction favoring the overlapping component.

Theorem 4.2 (Parameter Convergence). *Given (x, y) follows data distribution described in Section 3.2. For both the logistic regression and two-layer linear network, let T be the number of iterations w.r.t θ induced by GD (Eq. (1)), or w-step (Eq. (2)) and \mathbf{A} -step of AGD (Eq. (3)) with appropriate $\alpha, \alpha_1, \alpha_2 \preceq \sigma_{\parallel}^{-2}$; If:*

- $\|\theta_{\parallel}^{(T)} - \theta_{\parallel}^*\| \leq \delta$ then, $T = \Omega(\log(\|\theta^{(0)} - \theta_{\parallel}^*\| \cdot \delta^{-1}))$
- $\|\theta_{\perp}^{(T)} - \theta_{\perp}^*\| \leq \delta$ then, $T = \Omega((\sigma_{\parallel}/\sigma_{\perp})^2 \cdot \log(\|\theta^{(0)} - \theta_{\perp}^*\| \cdot \delta^{-1}))$

Theorem 4.2 provides the convergence rate in terms of the identifiable parameter θ in both \perp, \parallel directions. The convergence rate in the \parallel -direction is independent of the dimensionality, whereas for \perp -direction the rate depends on $(\sigma_{\perp}/\sigma_{\parallel})^{-1}$. Note that as $\sigma_{\perp}/\sigma_{\parallel} \rightarrow 0$ or $\sigma_{\perp} = 0$ (x_{\perp} follows a discrete distribution), the data distribution of x becomes a d -dimensional manifold immersed in D -dimension space and the time required for convergence in \perp -direction blows to ∞ .

Theorem 4.3 (Loss Convergence). *Given (x, y) follows data distribution described in Section 3.2. For both the logistic regression and two-layer linear network, let T be the number of iterations w.r.t θ induced by GD (Eq. (1)), or w-step (Eq. (2)) and \mathbf{A} -step of AGD (Eq. (3)) with appropriate $\alpha, \alpha_1, \alpha_2 \preceq \sigma_{\parallel}^{-2}$. If θ^* is the optimal solution, such that $(\mathcal{L}(\theta^{(T)}) - \mathcal{L}(\theta^*)) < \delta$; then:*

- $T = \min(r_1, r_2)$ if $\delta > C$.
- $T = r_2$ if $\delta < C$.

where $r_1 = \Omega(\log(|\mathcal{L}(\theta^{(0)}) - \mathcal{L}(\theta^*)| \cdot (\delta - C)^{-1}))$, $r_2 = \Omega((\sigma_{\parallel}/\sigma_{\perp})^2 \cdot \log(|\mathcal{L}(\theta^{(0)}) - \mathcal{L}(\theta^*)| \cdot \delta^{-1}))$ and $C = \Omega(\nu \log 2)$.

Theorem 4.3 provides the convergence rates in terms of the loss. Additionally, it states that if the error tolerance $\delta \gg C$, we can have fast convergence rate r_1 independent of dimensionality ($\sigma_{\perp}^2/\sigma_{\parallel}^2$). However, for an arbitrarily small $\delta < C$, the convergence rate r_2 can be significantly slower controlled by the dimensionality ($\sigma_{\perp}/\sigma_{\parallel}$) of the data. The threshold $C = \Omega(\nu \log 2)$ is essentially the minimum loss that can be attained by only training θ_{\parallel} (A.5). As $\delta \rightarrow C$, the rate r_2 depended on dimensionality takes over.

Well separated on-manifold distribution Suppose there is no overlap, i.e., $\nu = 0$, then Theorem 4.3 tells us that we can always have a fast convergence rate independent of dimensionality for any arbitrary error-tolerance δ . The on-manifold coefficients are sufficient for perfect classification, corresponding to faster convergence. In this scenario, as long as convergence in \parallel direction is attained, the data is perfectly classifiable. Hence, the classifier can achieve robustness just based on the on-manifold direction. (Fig 3b)

Illusion of convergence When ν is small, the model can attain fast convergence to a small loss value; however, to perfectly classify the data distribution, convergence in both \perp and \parallel direction is still required as $\nu > 0$ (Fig 3a). The model in this scenario will face adversarial vulnerability due to the poor convergence in the \perp direction, even though the loss value is small.

5 Towards second-order optimization

Based on our motivation (Section 4.1) and the proofs of the Theorems described in Section 4.2, the ill-conditioned nature of clean training is dictated by the usage of uniform small step size in both \parallel and \perp direction. A small step size in the \parallel direction is necessary due to large curvature, for careful descent. In the \perp direction, where curvature is small, larger steps could be taken for efficiency. Variable step sizes for each direction will address ill-conditioning, we can get convergence rates independent of dimensionality $\sigma_{\perp}/\sigma_{\parallel}$ for Theorems 4.2,4.3 in all cases. (Remark A.1) First-order methods can't automatically choose appropriate step sizes based on the curvature, but for the sake of argument, let us consider a second-order step like Newton's method instead of the GD step in Eq. (1).

$$\theta^{(t+1)} = \theta^{(t)} - \left(\nabla_{\theta}^2 \mathcal{L}(\theta^{(t)}) \right)^{-1} \nabla_{\theta} \mathcal{L}(\theta^{(t)}). \quad (8)$$

The inverse hessian in the above equation is analogous to the uniform step size α in GD. However, for Newton's method, the effective step size is controlled by the inverse of the curvature. Large curvature or sharp directions are traversed carefully, and small curvature or flat directions are traversed liberally. The usage of second-order methods automatically induces variable step size, circumventing the ill-conditioning.

Hessian Estimate In practice, computing the hessian inverse in Eq. (8) is computationally expensive. Hence, instead of using exact Hessians, we can use preconditioning matrices that approximate the Hessian inverse well. Our experiments use a relatively fast and inexpensive approximation to the hessian inverse known as the KFAC (Martens and Grosse, 2015) preconditioner. KFAC scales efficiently in a distributed

parallel setting for larger models. At its core, it is a natural gradient method that approximates the Fisher information as a layerwise block matrix and further approximates those blocks as being the Kronecker product of two much smaller matrices that are easier to compute.

6 Experiments

Most computer vision datasets can be attributed to having a low-dimensional manifold structure (Pope et al., 2021; Osher et al., 2017). According to our framework, if there is an overlap in the manifold dimensions, the clean training is subjected to ill-conditioning, requiring considerable time to converge. Consequently, if a lack of convergence leads to adversarial vulnerability, the robust accuracy should increase with enough training. Our discussions in Section 5, imply that with a second-order optimization scheme like KFAC, this robustness improvement should be much faster, and we could attain much more robust classifiers by just using clean training. We use the cross-entropy loss in our experiments, which is a multiclass generalization of the logistic loss we used in our theoretical setup.

We perform clean training on popular computer vision datasets MNIST (LeCun et al., 2010) and FashionMNIST (Xiao et al., 2017) with a convolution neural network models (Tables 1, 3, LeCun et al. (2015)) under two different optimization schemes first order and second order. We use the ADAM optimizer (Kingma and Ba, 2014), which is considered one of the fastest first-order methods. We incorporate KFAC preconditioned matrices for our second-order optimization into the existing ADAM update. We use pytorch implementations (Pauloski et al., 2020, 2021) to compute the KFAC preconditioning.

At each training epoch, we subject the model to adversarial attacks to keep track of the model’s robustness. We use ℓ_∞ Projected gradient descent (PGD)-attacks of strength ϵ to attack the models (Madry et al., 2017). The robust accuracy is evaluated on the test data unbeknownst to training for various choices of attack strength ϵ , where $\epsilon = 0$ corresponds to the clean test accuracy. The total training is limited to 1000 epochs for illustrative purposes. We implement 10 runs for each model to get the avg and std dev. After ~ 10 epochs, the clean training loss is ~ 0 in all scenarios. (For additional details see appendix B, Code:¹)

Figure 4 exhibits the results of our experiments de-

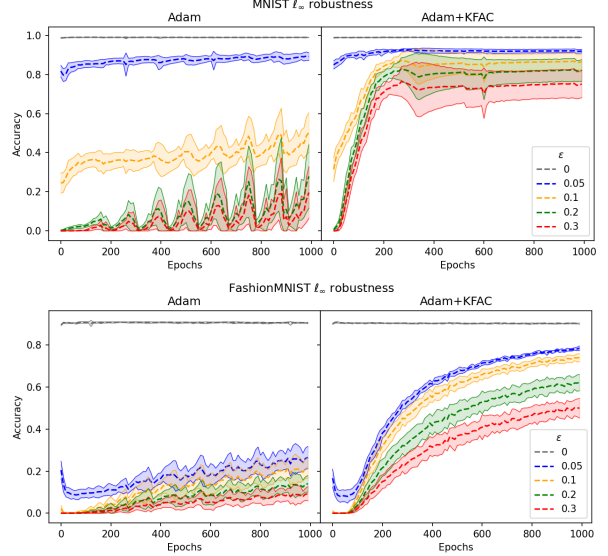


Figure 4: PGD ℓ_∞ robustness for clean MNIST (top)/FMNIST (bottom) model. Optimization Schemes (Left): First order ; (Right): Second Order.

scribed above for the MNIST and FMNIST datasets, respectively. It is evident that irrespective of the order of optimization, the robustness of the clean-trained model does increase with time under all attack strengths (ϵ) with time, as suggested by our theory. Even though the clean test accuracy is stagnant around ($\epsilon = 0$) is $\sim 100, \sim 95\%$ (MNIST, FMNIST resp.) for the majority of the training, the adversarial robustness increases throughout. This validates our theory, suggesting a lack of convergence in \perp direction leading to sub-optimal classifiers that aren’t large margin. Attaining, ~ 0 clean loss value and almost perfect test accuracy yet showcasing improvement in robustness throughout excessive training aligns with our discussions in section 4.2 (*Illusion of Convergence*) and the motivating illustration Fig 2 where the classifier is good enough on the data distribution, however, it hasn’t attained convergence to optimal classifier. Additionally, the rate of robustness improvement for the second-order optimization is much faster, for the same amount of training epochs.

Additionally, we conduct a similar robustness experiment on the CIFAR10 dataset (Krizhevsky et al., 2009) with ADAM training (Figure 5a). KFAC is designed to scale up in a distributed setting for larger models. Although we couldn’t provide the KFAC version for CIFAR10 due to limited access to a single GPU, we conducted the first-order training for larger epochs (4000) to illustrate robustness improvement. We expect a second-order optimization scheme would yield similar results but with much smaller training epochs, as observed in the MNIST and FashionMNIST cases.

¹https://anonymous.4open.science/r/Adv_Convergence_code-DF4B/

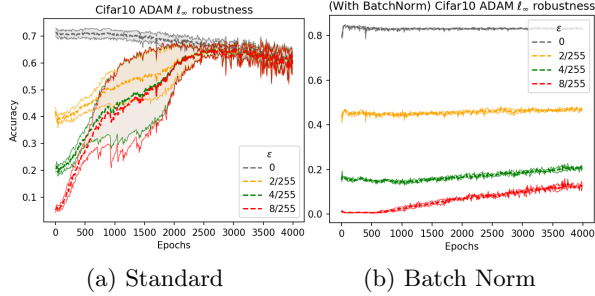


Figure 5: PGD ℓ_∞ robustness CIFAR10 clean model.

Unparalleled clean training performance Attaining ~ 80 and $\sim 40\%$ robust accuracy for $\epsilon = 0.3$ (ADAM+KFAC in Fig 4) in MNIST and FMNIST datasets respectively just by clean training is unprecedented. $\epsilon = 0.3$ is a very large attack strength for these datasets, for context Madry et al. (2017) reports a robust accuracy of only 3.5% for MNIST dataset undergoing clean training with the same attack strength. Similarly, for CIFAR10 Fig 5a, we attain $\sim 60\%$ robust accuracy for $\epsilon = 8/255$ just using clean training. Traditional literature reports 0% robust accuracy for clean-trained model and 47.04% accuracy for the PGD-based adversarially trained model (Zhang et al., 2019).

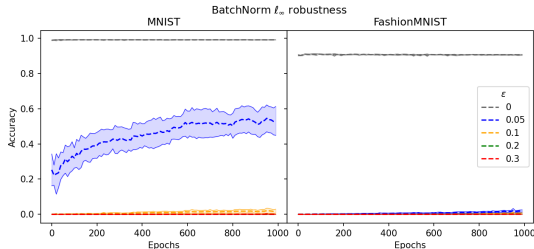


Figure 6: PGD ℓ_∞ robustness for clean MNIST (left), FMNIST (right) models with batch-norm layers.

6.1 Vulnerability of Batch-Normalization

Figures 6 and 5b plot identical experiments but with the model architectures, including batch-normalization (Table 2, 4). In this scenario, there is no robustness improvement with additional training, suggesting that batch-normalized models are vulnerable even at convergence. This aligns with the fact that contrary to traditional ReLU networks, which have an implicit bias towards maximum margin classifier, batch normalized networks have an implicit bias toward uniform margin (Cao et al., 2023). A uniform margin classifier doesn't enjoy the robustness properties of a maximum margin classifier due to its geometry. This raises robustness concerns for modern ML pipelines where batch normal-

ization is a default.

7 Discussion and Conclusion

We extend the notion of on and off-manifold dimensions to high and low-variance features. We explore a framework where inseparability in the on-manifold direction between classes causes adversarial vulnerability due to poor off-manifold learning from ill-conditioning. We present theoretical results supporting this hypothesis for a binary classification problem on a toy data distribution motivated by this concept. The theoretical analysis is done for the logistic regression case and 2-layer linear network for mathematical tractability. However, the idea of ill-conditioning facilitated by using first-order optimization for a model trained on a low-dimensional data manifold, resulting in adversarial vulnerability when data is inseparable in manifold direction, seems much more general. We verify this contrapositively by implementing experiments on MNIST, FMNIST, and CIFAR10 datasets with CNNs under a cross-entropy loss. Furthermore, we advocate using second-order methods that inherently circumvent ill-conditioning and lead us to a much more robust classifier just by using clean training.

Adversarial Training In practice, adversarial training (AT) is used to induce robustness in models (Goodfellow et al., 2014; Madry et al., 2017). Clean training minimizes the loss for original data distribution, whereas AT minimizes the loss for the distribution of perturbed data or adversarial examples. AT requires a parameter ϵ corresponding to the attack strength or search radius of adversarial examples from the original data distribution. Given, ϵ is less than the *margin* between the distinct classes, AT is doing clean training on the adversarial examples distribution. This forms an ϵ -ball cover around the original data distribution. Even if the original data distribution is low dimensional, the adversarial example distribution will be the exact ambient dimension. In our framework, this translates to the fact that the off-manifold or low variance features will also have an ϵ -ball cover, effectively increasing its variance. Hence, $\sigma_\perp/\sigma_\parallel$ increases from the original data distribution to the adversarial counterpart, thereby improving the convergence (Theorems 4.2, 4.3). This explains why adversarial training can find a robust classifier while clean training cannot, even though a robust classifier is also an optimal solution to the clean loss.

References

- Achour, E. M., Malgouyres, F., and Mamalet, F. (2022). Existence, stability and scalability of orthogonal convolutional neural networks. *Journal of Machine Learning Research*, 23(347):1–56.
- Alemany, S. and Pissinou, N. (2020). The dilemma between data transformations and adversarial robustness for time series application systems. *arXiv preprint arXiv:2006.10885*.
- Aparne, G., Banburski, A., and Poggio, T. (2022). Pca as a defense against some adversaries. Technical report, Center for Brains, Minds and Machines (CBMM).
- Boyd, S. P. and Vandenberghe, L. (2004). *Convex optimization*. Cambridge university press.
- Cao, Y., Zou, D., Li, Y., and Gu, Q. (2023). The implicit bias of batch normalization in linear models and two-layer linear convolutional neural networks.
- Carlini, N. and Wagner, D. (2017). Towards evaluating the robustness of neural networks. In *2017 IEEE Symposium on Security and Privacy (SP)*, pages 39–57. Ieee.
- Chen, Y., Huang, W., Nguyen, L., and Weng, T.-W. (2021). On the equivalence between neural network and support vector machine. *Advances in Neural Information Processing Systems*, 34:23478–23490.
- Domingos, P. (2020). Every model learned by gradient descent is approximately a kernel machine. *arXiv preprint arXiv:2012.00152*.
- Frei, S., Vardi, G., Bartlett, P., and Srebro, N. (2024). The double-edged sword of implicit bias: Generalization vs. robustness in relu networks. *Advances in Neural Information Processing Systems*, 36.
- Goodfellow, I., Bengio, Y., and Courville, A. (2016). *Deep Learning*. MIT Press. <http://www.deeplearningbook.org>.
- Goodfellow, I. J., Shlens, J., and Szegedy, C. (2014). Explaining and harnessing adversarial examples. *arXiv preprint arXiv:1412.6572*.
- Haldar, R., Xing, Y., and Song, Q. (2024). Effect of ambient-intrinsic dimension gap on adversarial vulnerability. In Dasgupta, S., Mandt, S., and Li, Y., editors, *Proceedings of The 27th International Conference on Artificial Intelligence and Statistics*, volume 238 of *Proceedings of Machine Learning Research*, pages 1090–1098. PMLR.
- Jha, S., Jang, U., Jha, S., and Jalaian, B. (2018). Detecting adversarial examples using data manifolds. In *MILCOM 2018-2018 IEEE Military Communications Conference (MILCOM)*, pages 547–552. IEEE.
- Kingma, D. P. and Ba, J. (2014). Adam: A method for stochastic optimization. *arXiv preprint arXiv:1412.6980*.
- Krizhevsky, A. et al. (2009). Learning multiple layers of features from tiny images.
- LeCun, Y., Bengio, Y., and Hinton, G. (2015). Deep learning. *nature*, 521(7553):436–444.
- LeCun, Y., Cortes, C., and Burges, C. (2010). Mnist handwritten digit database. *ATT Labs [Online]*. Available: <http://yann.lecun.com/exdb/mnist>, 2.
- Li, S., Jia, K., Wen, Y., Liu, T., and Tao, D. (2019). Orthogonal deep neural networks. *IEEE transactions on pattern analysis and machine intelligence*, 43(4):1352–1368.
- Lin, W.-A., Lau, C. P., Levine, A., Chellappa, R., and Feizi, S. (2020). Dual manifold adversarial robustness: Defense against lp and non-lp adversarial attacks. *Advances in Neural Information Processing Systems*, 33:3487–3498.
- Lindqvist, B., Sugrim, S., and Izmailov, R. (2018). Autogan: Robust classifier against adversarial attacks. *arXiv preprint arXiv:1812.03405*.
- Liu, J., Jiang, G., Bai, Y., Chen, T., and Wang, H. (2020). Understanding why neural networks generalize well through gsnr of parameters. *arXiv preprint arXiv:2001.07384*.
- Lyu, K. and Li, J. (2019). Gradient descent maximizes the margin of homogeneous neural networks. *arXiv preprint arXiv:1906.05890*.
- Lyu, K., Li, Z., Wang, R., and Arora, S. (2021). Gradient descent on two-layer nets: Margin maximization and simplicity bias.
- Madry, A., Makelov, A., Schmidt, L., Tsipras, D., and Vladu, A. (2017). Towards deep learning models resistant to adversarial attacks. *arXiv preprint arXiv:1706.06083*.
- Martens, J. and Grosse, R. (2015). Optimizing neural networks with kronecker-factored approximate curvature. In *International conference on machine learning*, pages 2408–2417. PMLR.
- Melamed, O., Yehudai, G., and Vardi, G. (2024). Adversarial examples exist in two-layer relu networks for low dimensional linear subspaces. *Advances in Neural Information Processing Systems*, 36.
- Min, H. and Vidal, R. (2024). Can implicit bias imply adversarial robustness? *arXiv preprint arXiv:2405.15942*.
- Nacson, M. S., Srebro, N., and Soudry, D. (2022). Stochastic gradient descent on separable data: Exact convergence with a fixed learning rate.

- Nesterov, Y. (2013). *Introductory lectures on convex optimization: A basic course*, volume 87. Springer Science & Business Media.
- Osher, S., Shi, Z., and Zhu, W. (2017). Low dimensional manifold model for image processing. *SIAM Journal on Imaging Sciences*, 10(4):1669–1690.
- Pauloski, J. G., Huang, Q., Huang, L., Venkataraman, S., Chard, K., Foster, I., and Zhang, Z. (2021). Kaisa: An Adaptive Second-Order Optimizer Framework for Deep Neural Networks. In *Proceedings of the International Conference for High Performance Computing, Networking, Storage and Analysis*, SC ’21, New York, NY, USA. Association for Computing Machinery.
- Pauloski, J. G., Zhang, Z., Huang, L., Xu, W., and Foster, I. T. (2020). Convolutional Neural Network Training with Distributed K-FAC. In *Proceedings of the International Conference for High Performance Computing, Networking, Storage and Analysis*, SC ’20. IEEE Press.
- Pope, P., Zhu, C., Abdelkader, A., Goldblum, M., and Goldstein, T. (2021). The intrinsic dimension of images and its impact on learning. *arXiv preprint arXiv:2104.08894*.
- Rosset, S., Zhu, J., and Hastie, T. (2003). Margin maximizing loss functions. *Advances in neural information processing systems*, 16.
- Shamir, A., Melamed, O., and BenShmuel, O. (2021). The dimpled manifold model of adversarial examples in machine learning. *arXiv preprint arXiv:2106.10151*.
- Stutz, D., Hein, M., and Schiele, B. (2019). Disentangling adversarial robustness and generalization. In *Proceedings of the IEEE/CVF Conference on Computer Vision and Pattern Recognition*, pages 6976–6987.
- Szegedy, C., Zaremba, W., Sutskever, I., Bruna, J., Erhan, D., Goodfellow, I., and Fergus, R. (2013). Intriguing properties of neural networks. *arXiv preprint arXiv:1312.6199*.
- Wei, C., Lee, J. D., Liu, Q., and Ma, T. (2019). Regularization matters: Generalization and optimization of neural nets vs their induced kernel. *Advances in Neural Information Processing Systems*, 32.
- Xiao, H., Rasul, K., and Vollgraf, R. (2017). Fashion-mnist: a novel image dataset for benchmarking machine learning algorithms.
- Xiao, J., Yang, L., Fan, Y., Wang, J., and Luo, Z.-Q. (2022). Understanding adversarial robustness against on-manifold adversarial examples. *arXiv preprint arXiv:2210.00430*.
- Zhang, H., Yu, Y., Jiao, J., Xing, E., El Ghaoui, L., and Jordan, M. (2019). Theoretically principled trade-off between robustness and accuracy. In *International conference on machine learning*, pages 7472–7482. PMLR.
- Zhang, W., Zhang, Y., Hu, X., Goswami, M., Chen, C., and Metaxas, D. N. (2022). A manifold view of adversarial risk. In *International Conference on Artificial Intelligence and Statistics*, pages 11598–11614. PMLR.

A Proofs

In all our proofs, we assume that $\text{Rank}(\mathbf{A}) = D$, as when $\text{Rank}(\mathbf{A}) < D$, we can just work with a block of \mathbf{A} that is full rank. The gradient of w corresponding to the co-kernel of \mathbf{A} will always be zero, and it doesn't affect any of the gradient descent steps pertaining to our analysis.

A.1 Reparametrization

Lemma A.1.1 (Reparametrization). *For the t^{th} iterate of w -step Eq. (2) and \mathbf{A} -step of AGD Eq. (3) there exist reparametrizations $\tilde{w}^{(t)}$ and $\tilde{\mathbf{A}}^{(t)}$ such that $\theta^{(2t+1)} = (\theta_{\parallel}^{(2t+1)}, \theta_{\perp}^{(2t+1)}) = (\tilde{a}_{\parallel}^{(t)}, \tilde{a}_{\perp}^{(t)})$ and $\theta^{(2t)} = (\theta_{\parallel}^{(2t)}, \theta_{\perp}^{(2t)}) = (\tilde{w}_{\parallel}^{(t)}, \tilde{w}_{\perp}^{(t)})$. Where $\tilde{w} = (\tilde{w}_{\parallel}, \tilde{w}_{\perp}, \tilde{w}_{\vdash})$, $\text{vec } \tilde{\mathbf{A}} = (\tilde{a}_{\parallel}, \tilde{a}_{\perp}, \tilde{a}_{\vdash})$ and $\nabla \mathcal{L}_{\tilde{w}_{\vdash}} = \mathbf{0}_{m-D}$, $\nabla \mathcal{L}_{\tilde{a}_{\vdash}} = \mathbf{0}_{mD-D}$.*

Proof. Recall that, for the two-layer linear network, $\gamma = (\text{vec } \mathbf{A}, w)$ and $\theta = \mathbf{A}^T w$, with $\nabla_{\theta} \mathcal{L}(\gamma) = -\mathbb{E}_{\sim x, y} yx\sigma(-y \cdot z)$ (Eq. (4)). Our reparametrization/change of basis will help us separate the components of the first and second layer into \parallel, \perp, \vdash directions corresponding to the identifiable parameter $\theta = (\theta_{\parallel}, \theta_{\perp})$. \vdash components correspond to redundant directions that don't undergo any change in the AGD step.

A.1.1 w -step

In this step of AGD, the second layer is fixed to $\mathbf{A}^{(t)}$. Given $\mathbf{A} = \mathbf{A}^{(t)}$, the gradient w.r.t. the first layer parameter w is:

$$\nabla_w \mathcal{L}(\theta^{(2t)}) = -\mathbb{E} \sigma(-y \cdot z) y \mathbf{A} x \quad (9)$$

\mathbf{A} is a rectangular matrix ($m \times D; m \geq D$). $\text{Rank}(\mathbf{A}) \leq D$. Hence there exists a change of basis $\mathbf{B} \in \mathbb{R}^{m \times m}$ such that $\mathbf{A} = \mathbf{B}[\mathbf{e}_1 \dots \mathbf{e}_D]$ where \mathbf{e}_i is the standard basis in \mathbb{R}^m with i^{th} coordinate being 1, and rest 0. This choice of standard basis for the $\text{Im}(\mathbf{A})$ loses no generality as we can always have $\tilde{\mathbf{B}} = \mathbf{B}\mathbf{P}$ which permutes the basis in such a way so that the transformation adheres to the choice of a subset of the standard basis. In general $\mathbf{B} = [\mathbf{A} \quad \mathbf{C}]$ has to take this kind of form, for any choice of $\mathbf{C} \in \mathbb{R}^{m \times m-D}$. Hence, the gradient w.r.t. can be expressed as:

$$\nabla_w \mathcal{L}(\theta^{(2t)}) = -\mathbb{E} \sigma(-y \cdot z) y \mathbf{B} \begin{pmatrix} x \\ \mathbf{0}_{m-D} \end{pmatrix} \quad (10)$$

We can choose an appropriate full rank \mathbf{C} outside the span of \mathbf{B} to get an inverse transformation \mathbf{B}^{-1} . Note in the case that $\text{Rank}(\mathbf{A}) < D$ we can just work with block inverse of the full rank part in \mathbf{B} ; as the gradient of w corresponding to the co-kernel of \mathbf{A} will always be zero, so it isn't of interest.

Consider the reparametrization $\tilde{w}^{(t)} = \mathbf{B}^T w^{(t)}$, with gradients:

$$\nabla_{\tilde{w}} \mathcal{L}(\theta^{(2t)}) = \mathbf{B}^{-1} \nabla_w \mathcal{L} = -\mathbb{E} \sigma(-y \cdot z) y \mathbf{A} x = -\mathbb{E} \sigma(-y \cdot z) y \begin{pmatrix} x \\ \mathbf{0}_{m-D} \end{pmatrix} \quad (11)$$

Note that, $\theta^{(2t)} = \mathbf{A}^{(t)T} w^{(t)} = (\mathbf{B}[\mathbf{e}_1 \dots \mathbf{e}_D])^T w^{(t)} = [\mathbf{e}_1 \dots \mathbf{e}_D]^T \tilde{w}^{(t)}$. Therefore, it follows that there exists $\tilde{w}_{\parallel}, \tilde{w}_{\perp}$ components corresponding to $\theta_{\parallel}, \theta_{\perp}$ at every t . Note that the remaining components \tilde{w}_{\vdash} are redundant and have zero gradients.

$$\nabla_{\tilde{w}} \mathcal{L}(\theta) = -\mathbb{E} \sigma(-y \cdot z) y \begin{pmatrix} x \\ \mathbf{0}_{m-D} \end{pmatrix} \quad (12)$$

$$\nabla_{\tilde{w}_{\parallel}} \mathcal{L}(\theta) = -\mathbb{E} \sigma(-y \cdot z) y x_{\parallel} \quad (13)$$

$$\nabla_{\tilde{w}_{\perp}} \mathcal{L}(\theta) = -\mathbb{E} \sigma(-y \cdot z) y x_{\perp} \quad (14)$$

$$\nabla_{\tilde{w}_{\vdash}} \mathcal{L}(\theta) = \mathbf{0}_{m-D} \quad (15)$$

A.1.2 \mathbf{A} -step

In this step, the first layer is fixed to $w^{(t+1)}$. Given $w = w^{(t+1)}$, the gradient w.r.t. the second layer parameters \mathbf{A} is :

$$\nabla_{\mathbf{A}} \mathcal{L} = -\mathbb{E} \sigma(-y \cdot z) y w x^T \quad (16)$$

$$\nabla_{\text{vec } \mathbf{A}} \mathcal{L} = -\mathbb{E} \sigma(-y \cdot z) y w \otimes x \quad (17)$$

Consider the reparametrization $\tilde{\mathbf{A}}$ such that $\mathbf{A}^{(t)} = \mathbf{U}^T \tilde{\mathbf{A}}^{(t)} = \begin{pmatrix} u_1 \\ \vdots \\ u_m \end{pmatrix}^T \tilde{\mathbf{A}}$. The columns are chosen using Gram-Schmidt such that, $u_1 = w/\|w\|^2$ and $\langle u_j, w \rangle = 0, \|u_j\| = 1$ for all $j \neq 1$. The gradient in the re-parametrized space is then:

$$\nabla_{\tilde{\mathbf{A}}} \mathcal{L} = -\mathbb{E} \sigma(-y \cdot z) y \mathbf{U} w x^T = -\mathbb{E} \sigma(-y \cdot z) y \mathbf{e}_1 x^T \quad (18)$$

$$\nabla_{\text{vec } \tilde{\mathbf{A}}} \mathcal{L} = -\mathbb{E} \sigma(-y \cdot z) y \mathbf{e}_1 \otimes x \quad (19)$$

Note that,

$$\theta^{(2t+1)} = \mathbf{A}^{(t)T} w^{(t+1)} = (\mathbf{U}^T \tilde{\mathbf{A}}^{(t)})^T w^{t+1} = \tilde{\mathbf{A}}^{(t)T} \mathbf{U} w^{t+1} = \tilde{\mathbf{A}}^{(t)T} \mathbf{e}_1$$

. Therefore, it follows that there exists $a_{||}, a_{\perp}$ components for $\text{vec } \tilde{\mathbf{A}}$ corresponding to $\theta_{||}, \theta_{\perp}$ at every t . Hence, $\text{vec } \tilde{\mathbf{A}} = (a_{||}, a_{\perp}, a_{\perp})$ with:

$$\nabla_{a_{||}} \mathcal{L}(\theta) = -\mathbb{E} \sigma(-y \cdot z) y x_{||} \quad (20)$$

$$\nabla_{a_{\perp}} \mathcal{L}(\theta) = -\mathbb{E} \sigma(-y \cdot z) y x_{\perp} \quad (21)$$

$$\nabla_{a_{\perp}} \mathcal{L}(\theta) = \mathbf{0}_{mD-D} \quad (22)$$

□

A.2 Hessian

Lemma A.2.1 (Lipschitz smoothness and Strong Convexity). *For any value of γ in both logistic and two-layer-linear setting. The loss Hessians w.r.t. identifiable parameter θ can be bounded as follows:*

$$c_l \cdot \begin{pmatrix} \sigma_{||}^2 \mathbf{I}_d & \mathbf{0} \\ \mathbf{0} & \sigma_{\perp}^2 \mathbf{I}_g \end{pmatrix} < \nabla_{\theta}^2 \mathcal{L}(\gamma) < c_u \cdot \begin{pmatrix} \sigma_{||}^2 \mathbf{I}_d & \mathbf{0} \\ \mathbf{0} & \sigma_{\perp}^2 \mathbf{I}_g \end{pmatrix} \quad (23)$$

$$c_l \sigma_{\perp}^2 \mathbf{I}_g < \nabla_{\theta_{\perp}}^2 \mathcal{L}(\gamma) < c_u \sigma_{\perp}^2 \mathbf{I}_g \quad (24)$$

$$c_l \sigma_{||}^2 \mathbf{I}_d < \nabla_{\theta_{||}}^2 \mathcal{L}(\gamma) < c_u \sigma_{||}^2 \mathbf{I}_d \quad (25)$$

Here $c_l, c_u > 0$ are constants. Consequently, $\mathcal{L}(\gamma)$ is convex in $\theta, \theta_{||}, \theta_{\perp}$.

Proof. The Hessian of the loss w.r.t. the identifiable parameter θ is $\nabla_{\theta}^2 \mathcal{L}(\gamma) = \mathbb{E}_{x,y} x x^T \sigma(z) \sigma(-z)$ [Eq. (5)].

As our analysis is restricted to the compact space, $\sigma(z)$ is strictly between 0 and 1, as $\sigma(z) = 1/0$ if and only if $\theta = \pm\infty$. Let $c_l > 0$ be the lower bound of the entropy $\sigma(z)\sigma(-z)$. Then, using positive definiteness and integrating both sides (Here $>, <$ between matrices corresponds to the difference being positive/negative definite):

$$\begin{aligned} \mathbb{E}_{x,y} x x^T c_l &< \nabla_{\theta}^2 \mathcal{L}(\gamma) < \mathbb{E}_{x,y} x x^T \\ (\Sigma_x + \mathbb{E}_{x,y} x \mathbb{E}_{x,y} x^T) \cdot c_l &< \nabla_{\theta}^2 \mathcal{L}(\gamma) < \Sigma_x + \mathbb{E}_{x,y} x \mathbb{E}_{x,y} x^T \end{aligned}$$

Where $\Sigma_x = \begin{pmatrix} \sigma_{||}^2 \mathbf{I}_d & \mathbf{0} \\ \mathbf{0} & \sigma_{\perp}^2 \mathbf{I}_g \end{pmatrix}$ is the covariance matrix. The vector outer-product $\mathbb{E} x \mathbb{E} x^T$ has eigenvalues $\|\mu\|^2 = \|\mathbb{E} x\|^2, 0, 0, \dots, 0$. Hence, $\mathbf{0}_D \leq \mathbb{E} x \mathbb{E} x^T \leq \|\mu\|^2 \mathbf{I}_D$. This implies that:

$$\Sigma_x \cdot c_l < \nabla_{\theta}^2 \mathcal{L}(\gamma) < \Sigma_x + \|\mu\|^2 \mathbf{I}_D$$

For $0 < \|\mu\|, \sigma_{||}, \sigma_{\perp} < \infty$. We have $\|\mu\| = c_{||} \sigma_{||} = c_{\perp} \sigma_{\perp}$

$$c_l \cdot \begin{pmatrix} \sigma_{||}^2 \mathbf{I}_d & \mathbf{0} \\ \mathbf{0} & \sigma_{\perp}^2 \mathbf{I}_g \end{pmatrix} < \nabla_{\theta}^2 \mathcal{L}(\gamma) < \begin{pmatrix} \sigma_{||}^2 \mathbf{I}_d & \mathbf{0} \\ \mathbf{0} & \sigma_{\perp}^2 \mathbf{I}_g \end{pmatrix} + \begin{pmatrix} c_{||}^2 \sigma_{||}^2 \mathbf{I}_d & \mathbf{0} \\ \mathbf{0} & c_{\perp}^2 \sigma_{\perp}^2 \mathbf{I}_g \end{pmatrix}$$

Then there exists constants $c_u = \max\{1 + c_{||}^2, 1 + c_{\perp}^2\}$ such that

$$c_l \cdot \begin{pmatrix} \sigma_{||}^2 \mathbf{I}_d & \mathbf{0} \\ \mathbf{0} & \sigma_{\perp}^2 \mathbf{I}_g \end{pmatrix} < \nabla_{\theta}^2 \mathcal{L}(\gamma) < c_u \cdot \begin{pmatrix} \sigma_{||}^2 \mathbf{I}_d & \mathbf{0} \\ \mathbf{0} & \sigma_{\perp}^2 \mathbf{I}_g \end{pmatrix}$$

$$\begin{aligned} c_l \sigma_{\perp}^2 \mathbf{I}_g &< \nabla_{\theta_{\perp}}^2 \mathcal{L}(\gamma) < c_u \sigma_{\perp}^2 \mathbf{I}_g \\ c_l \sigma_{\parallel}^2 \mathbf{I}_d &< \nabla_{\theta_{\parallel}}^2 \mathcal{L}(\gamma) < c_u \sigma_{\parallel}^2 \mathbf{I}_d \end{aligned}$$

As the above Hessians are positive definite, convexity follows. \square

Proof of Theorem 4.1. A.3 Gradient Decomposition

From Eq. (4) $\nabla_{\theta} \mathcal{L}(\gamma) = - \mathbb{E}_{\sim x, y} y x \sigma(-y \cdot z)$. We will tackle the \parallel / \perp components of the gradient separately.

A.3.1 On Manifold

Consider $\nabla_{\theta_{\parallel}} \mathcal{L}(\gamma) = - \mathbb{E}_{\sim x, y} y x_{\parallel} \sigma(-y \cdot z)$. $\nabla_{\theta_{\parallel}} \mathcal{L}$ can be decomposed into $\nabla_{\theta_{\parallel}} \mathcal{L}^{-\emptyset}, \nabla_{\theta_{\parallel}} \mathcal{L}^{\emptyset}$, the gradients arising from overlapping and non-overlapping distribution of x_{\parallel} , with probabilities $\nu, 1 - \nu$ respectively. The distribution of x corresponding to the non-overlapping part and overlapping part is $x_{\parallel}|_{y, \emptyset} \sim \mathcal{U}[0, (l - k) \cdot y \cdot \mathbb{1}_d]$ and $x_{\parallel}|_{y, -\emptyset} \sim \mathcal{U}[-k \cdot y \cdot \mathbb{1}_d, 0]$ resp. One can validate this with the definition of ν (Section 3.2), $x_{\parallel}|_{y, \emptyset}$ contributes 0 in the computation of ν , while $x_{\parallel}|_{y, -\emptyset}$ has non-zero contribution over the support.

$$\nabla_{\theta_{\parallel}} \mathcal{L}(\gamma) = - \mathbb{E}_{\sim x, y} y x_{\parallel} \sigma(-y \cdot z) = -(1 - \nu) \cdot \mathbb{E}_{\sim x, y| \emptyset} y x_{\parallel} \sigma(-y \cdot z) - \nu \cdot \mathbb{E}_{\sim x, y| -\emptyset} y x_{\parallel} \sigma(-y \cdot z) \quad (26)$$

$$\mathbb{E}_{\sim x, y| \emptyset} y x_{\parallel} \sigma(-y \cdot z) = \pi \cdot \mathbb{E}_{\sim x| y=1, \emptyset} x_{\parallel} \sigma(-z) + (1 - \pi) \cdot \mathbb{E}_{\sim x| y=-1, \emptyset} -x_{\parallel} \sigma(z) \quad (27)$$

$$\mathbb{E}_{\sim x| y=1, \emptyset} x_{\parallel} \sigma(-z) = \left[\int_0^{l-k} \cdots \int_0^{l-k} x_{\parallel i} \sigma(-z) \cdot (l - k)^{-d} dx \right]_{i \in \{1, \dots, d\}} \quad (28)$$

$$= \vec{c}_1 \odot \mathbb{1}_{d, l-k/2} \quad (29)$$

In Eq. (28) every integral is in a positive domain, with $\sigma(-z) \in (0, 1)$ within the compact space. $0 < \int_0^{l-k} x_{\parallel i} \sigma(-\theta_{\parallel i} x_{\parallel i}) < \int_0^{l-k} x_{\parallel i} = l-k/2$, component-wise we get Eq. (29) where $0 < \vec{c}_1 < 1$ for $i \in \{1, \dots, d\}$.

$$\begin{aligned} \mathbb{E}_{\sim x| y=-1, \emptyset} -x_{\parallel} \sigma(z) &= \left[\int_{-(l-k)}^0 \cdots \int_{-(l-k)}^0 -x_{\parallel i} \sigma(z) \cdot (l - k)^{-d} dx \right]_{i \in \{1, \dots, d\}} \\ &= \left[\int_0^{-(l-k)} \cdots \int_0^{-(l-k)} x_{\parallel i} \sigma(z) \cdot (l - k)^{-d} dx \right] \\ &= \left[\int_0^{l-k} \cdots \int_0^{l-k} x_{\parallel i} \sigma(-z) \cdot (l - k)^{-d} dx \right] \stackrel{\text{Eq. (28)}}{=} \vec{c}_1 \odot \mathbb{1}_{d, l-k/2} \end{aligned} \quad (30)$$

Substituting Eq. (29) and Eq. (30) in Eq. (27) we have:

$$\mathbb{E}_{\sim x, y| \emptyset} y x_{\parallel} \sigma(-y \cdot z) = \vec{c}_1 \odot \mathbb{1}_{d, l-k/2} \quad (31)$$

$$\mathbb{E}_{\sim x| y=1, -\emptyset} x_{\parallel} \sigma(-z) = \left[\int_{-k}^0 \cdots \int_{-k}^0 x_{\parallel i} \sigma(-z) \cdot k^{-d} dx \right]_{i \in \{1, \dots, d\}} \quad (32)$$

Using analogous arguments as in Eq. (28)

$$= -\vec{c}_2 \odot \mathbb{1}_{d, k/2} \quad (33)$$

Similarly, we have

$$\mathbb{E}_{\sim x| y=-1, -\emptyset} -x_{\parallel} \sigma(z) = -\vec{c}_2 \odot \mathbb{1}_{d, k/2} \quad (34)$$

Substitute Eq. (33) and Eq. (34) in

$$\mathbb{E}_{\sim x, y| -\emptyset} y x_{\parallel} \sigma(-y \cdot z) = \pi \cdot \mathbb{E}_{\sim x| y=1, -\emptyset} x_{\parallel} \sigma(-z) + (1 - \pi) \cdot \mathbb{E}_{\sim x| y=-1, -\emptyset} -x_{\parallel} \sigma(z) \quad (35)$$

to get

$$\mathbb{E}_{\sim x, y| -\emptyset} y x_{\parallel} \sigma(-y \cdot z) = -\vec{c}_2 \odot \mathbb{1}_{d, k/2} \quad (36)$$

Using Eq. (31), Eq. (36) in Eq. (26) we have:

$$\nabla_{\theta_{\parallel}} \mathcal{L}(\gamma) = -(1 - \nu) \cdot \vec{c}_1 \odot \mathbb{1}_{d, l-k/2} + \nu \cdot \vec{c}_2 \odot \mathbb{1}_{d, k/2} \quad (37)$$

A.3.2 Off Manifold

$$\nabla_{\theta_{\perp}} \mathcal{L}(\gamma) = - \mathbb{E}_{\sim x, y} y x_{\perp} \sigma(-y \cdot z) = -\pi \cdot \mathbb{E}_{\sim x|y=1} x_{\perp} \sigma(-z) - (1 - \pi) \cdot \mathbb{E}_{\sim x|y=-1} -x_{\perp} \sigma(z) \quad (38)$$

$$\mathbb{E}_{\sim x|y=1} x_{\perp} \sigma(-z) = \left[\int_{\mu_{\perp}^{(1)} - \sqrt{3}\sigma_{\perp}}^{\mu_{\perp}^{(1)} + \sqrt{3}\sigma_{\perp}} \cdots \int_{\mu_{\perp}^{(1)} - \sqrt{3}\sigma_{\perp}}^{\mu_{\perp}^{(1)} + \sqrt{3}\sigma_{\perp}} x_{\perp} \sigma(-z) \cdot (2\sqrt{3}\sigma_{\perp})^{-g} dx \right] dx, \quad i \in \{1, \dots, g\} \quad (39)$$

Let $x_{\perp} = \mu_{\perp}^{(1)} + \eta$, then

$$\begin{aligned} &= \left[\int_{-\sqrt{3}\sigma_{\perp}}^{\sqrt{3}\sigma_{\perp}} \cdots \int_{-\sqrt{3}\sigma_{\perp}}^{\sqrt{3}\sigma_{\perp}} (\mu_{\perp}^{(1)} + \eta)_i \sigma(-z) \cdot (2\sqrt{3}\sigma_{\perp})^{-g} d\eta \right] \\ &= \vec{c}_3 \odot \mu_{\perp}^{(1)} + \left[\int_0^{\sqrt{3}\sigma_{\perp}} \cdots \int_0^{\sqrt{3}\sigma_{\perp}} \eta_i \sigma(-z) \cdot (2\sqrt{3}\sigma_{\perp})^{-g} d\eta \right] \\ &+ \left[\int_{-\sqrt{3}\sigma_{\perp}}^0 \cdots \int_{-\sqrt{3}\sigma_{\perp}}^0 \eta_i \sigma(-z) \cdot (2\sqrt{3}\sigma_{\perp})^{-g} d\eta \right] \\ &= \vec{c}_3 \odot \mu_{\perp}^{(1)} + (\vec{c}_4 + \vec{c}_5) \odot \mathbb{1}_g \cdot \sigma_{\perp}/4 \end{aligned} \quad (40)$$

Also,

$$\mathbb{E}_{\sim x|y=-1} -x_{\perp} \sigma(z) = \mathbb{E}_{\sim x|y=-1} -x_{\perp} + \mathbb{E}_{\sim x|y=-1} x_{\perp} \sigma(-z)$$

Following similar steps following Eq. (39) to Eq. (40)

$$= -\mu_{\perp}^{(-1)} + \vec{c}_6 \odot \mu_{\perp}^{(-1)} + (\vec{c}_4 + \vec{c}_5) \odot \mathbb{1}_g \cdot \sigma_{\perp}/4 \quad (41)$$

Substituting Eq. (40), Eq. (41) in Eq. (38) we have:

$$\nabla_{\theta_{\perp}} \mathcal{L}(\gamma) = -\pi \left(\vec{c}_3 \odot \mu_{\perp}^{(1)} \right) - (1 - \pi) \left(-(\mathbb{1}_g - \vec{c}_6) \odot \mu_{\perp}^{(-1)} \right) - (\vec{c}_4 + \vec{c}_5) \odot \mathbb{1}_g \cdot \sigma_{\perp}/4$$

A.4 Progressive Bound

A.4.1 Loss change all directions

$\Delta \mathcal{L}(t) = \mathcal{L}(\theta^{(t+1)}) - \mathcal{L}(\theta^{(t)})$. Using Taylor's expansion of $\mathcal{L}(\theta^{(t+1)})$ around $\theta^{(t)}$ with Lipschitz smoothness Eq. (23), we have:

$$\mathcal{L}(\theta^{(t+1)}) < \mathcal{L}(\theta^{(t)}) + \nabla_{\theta} \mathcal{L}(\theta^{(t)})^T (\theta^{(t+1)} - \theta^{(t)}) + \frac{c_u}{2} (\theta^{(t+1)} - \theta^{(t)})^T \begin{pmatrix} \sigma_{\parallel}^2 \mathbf{I}_d & \mathbf{0} \\ \mathbf{0} & \sigma_{\perp}^2 \mathbf{I}_g \end{pmatrix} (\theta^{(t+1)} - \theta^{(t)})$$

As $\sigma_{\perp} < \sigma_{\parallel}$, we have:

$$\mathcal{L}(\theta^{(t+1)}) < \mathcal{L}(\theta^{(t)}) + \nabla_{\theta} \mathcal{L}(\theta^{(t)})^T (\theta^{(t+1)} - \theta^{(t)}) + \frac{c_u}{2} (\theta^{(t+1)} - \theta^{(t)})^T \sigma_{\parallel}^2 \mathbf{I}_D (\theta^{(t+1)} - \theta^{(t)})$$

1. For **logistic case** the gradient step is $\theta^{(t+1)} = \theta^{(t)} - \alpha \nabla_{\theta} \mathcal{L}(\theta^{(t)})$

$$\begin{aligned} \mathcal{L}(\theta^{(t+1)}) &< \mathcal{L}(\theta^{(t)}) - \alpha \|\nabla_{\theta} \mathcal{L}(\theta^{(t)})\|^2 + \alpha^2 \frac{c_u \sigma_{\parallel}^2}{2} \|\nabla_{\theta} \mathcal{L}(\theta^{(t)})\|^2 \\ \Delta \mathcal{L}(t) &< -\alpha \|\nabla_{\theta} \mathcal{L}(\theta^{(t)})\|^2 \left(1 - \alpha \cdot \frac{c_u \sigma_{\parallel}^2}{2} \right) \end{aligned}$$

For step-size

$$\alpha \leq \frac{1}{c_u \sigma_{\parallel}^2} \quad (42)$$

$$\Delta \mathcal{L}(t) < -(2c_u \sigma_{\parallel}^2)^{-1} \|\nabla_{\theta} \mathcal{L}(\theta^{(t)})\|^2$$

2. For **w-step** Eq. (2) we have $w^{(t/2+1)} = w^{(t/2)} - \alpha_1 \nabla_w \mathcal{L}(\theta^{(t)})$. From lemma A.1.1, section:A.1.1 we have reparametrization $(\theta, \mathbf{0}_{m-D}) = \tilde{w}^{(t/2)} = \mathbf{B}^T w^{(t/2)}$. Note that $\mathbf{B} = [\mathbf{A}^{(t/2)} \quad \mathbf{C}]$ for some specific choice of \mathbf{C} . This induces a gradient descent step in \tilde{w} or θ space as follows $\tilde{w}^{(t/2+1)} = \tilde{w}^{(t/2)} - \alpha_1 \mathbf{B}^T \mathbf{B} \nabla_{\tilde{w}} \mathcal{L}(\theta^{(t)})$ or $\theta^{(t+1)} = \theta^{(t)} - \alpha_1 \mathbf{A}^{(t/2)T} \mathbf{A}^{(t/2)} \nabla_{\theta} \mathcal{L}(\theta^{(t)})$. Hence, the Taylor expansion can be written as:

$$\mathcal{L}(\theta^{(t+1)}) < \mathcal{L}(\theta^{(t)}) - \alpha_1 \nabla_{\theta} \mathcal{L}(\theta^{(t)})^T \mathbf{A}^{(t/2)T} \mathbf{A}^{(t/2)} \nabla_{\theta} \mathcal{L}(\theta^{(t)}) + \alpha_1^2 \frac{c_u \sigma_{\parallel}^2}{2} \|\mathbf{A}^{(t/2)T} \mathbf{A}^{(t/2)} \nabla_{\theta} \mathcal{L}(\theta^{(t)})\|^2$$

let $\hat{\lambda}_{\mathbf{A}}, \check{\lambda}_{\mathbf{A}}$ be the minimum/maximum eigen values of $\mathbf{A}^{(t/2)T} \mathbf{A}^{(t/2)}$ respectively. Then :

$$\begin{aligned} \mathcal{L}(\theta^{(t+1)}) &< \mathcal{L}(\theta^{(t)}) - \alpha_1 \hat{\lambda}_{\mathbf{A}} \|\nabla_{\theta} \mathcal{L}(\theta^{(t)})\|^2 + \alpha_1^2 \frac{c_u \sigma_{\parallel}^2}{2} \check{\lambda}_{\mathbf{A}}^2 \|\nabla_{\theta} \mathcal{L}(\theta^{(t)})\|^2 \\ \Delta \mathcal{L}(t) &< -\alpha_1 \cdot \hat{\lambda}_{\mathbf{A}} \|\nabla_{\theta} \mathcal{L}(\theta^{(t)})\|^2 \left(1 - \alpha_1 \cdot \frac{\check{\lambda}_{\mathbf{A}}^2 c_u \sigma_{\parallel}^2}{2 \hat{\lambda}_{\mathbf{A}}} \right) \end{aligned}$$

For step-size

$$\alpha_1 \leq (M \cdot c_u \sigma_{\parallel}^2)^{-1} \quad (43)$$

Where $\check{\lambda}_{\mathbf{A}}^2 / \hat{\lambda}_{\mathbf{A}} \leq M$ for all t and some $M < \infty$ (compact space).

$$\Delta \mathcal{L}(t) < -\hat{\lambda}_{\mathbf{A}} \cdot (2M \cdot c_u \sigma_{\parallel}^2)^{-1} \|\nabla_{\theta} \mathcal{L}(\theta^{(t)})\|^2$$

3. For **A-step** Eq. (3) we have $\mathbf{A}^{(t+1/2)} = \mathbf{A}^{(t-1/2)} - \alpha_2 \nabla_{\mathbf{A}} \mathcal{L}(\theta^{(t)})$. From lemma A.1.1, section A.1.2; $\text{vec } \mathbf{A}^{(t-1/2)} = \text{vec } \mathbf{U}^T \tilde{\mathbf{A}}^{(t-1/2)} = (\mathbf{I}_D \otimes \mathbf{U}^T) \text{vec } \tilde{\mathbf{A}}^{(t-1/2)}$. Let $\mathbf{K}^T = (\mathbf{I}_D \otimes \mathbf{U}^T)^{-1} = \mathbf{I}_D \otimes \text{Diag}(\|w^{(t+1/2)}\|^2, 1, \dots, 1) \mathbf{U}$ as $\mathbf{U}^T \text{Diag}(\|w^{(t+1/2)}\|^2, 1, \dots, 1) \mathbf{U} = \mathbf{I}_m$. This induces a gradient descent step in $\text{vec } \tilde{\mathbf{A}}$ or θ space as follows $\text{vec } \tilde{\mathbf{A}}^{(t+1/2)} = \text{vec } \tilde{\mathbf{A}}^{(t-1/2)} - \alpha_2 \mathbf{K}^T \mathbf{K} \nabla_{\tilde{\mathbf{A}}} \mathcal{L}(\theta^{(t)})$ (where $\mathbf{K}^T \mathbf{K} = \mathbf{I}_D \otimes \text{Diag}(\|w^{(t+1/2)}\|^4, 1, \dots, 1) \mathbf{I}_m$) or $\theta^{(t+1)} = \theta^{(t)} - \alpha_2 \|w^{(t+1/2)}\|^4 \nabla_{\theta} \mathcal{L}(\theta^{(t)})$. Following analogous steps to the derivation for the logistic case (Item 1), with step size

$$\alpha_2 = (W \cdot c_u \sigma_{\parallel}^2)^{-1} \quad (44)$$

, where $\|w^{(t+1/2)}\|^4 < W$ for all t . We get the following:

$$\Delta \mathcal{L}(t) < -\|w^{(t+1/2)}\|^4 \cdot (2 \cdot W c_u \sigma_{\parallel}^2)^{-1} \|\nabla_{\theta} \mathcal{L}(\theta^{(t)})\|^2$$

A.4.2 Loss change on-manifold direction

$\Delta_{\parallel} \mathcal{L}(t) = \mathcal{L}(\theta_{\parallel}^{(t+1)}, \theta_{\perp}^{(t)}) - \mathcal{L}(\theta^{(t)})$. Using Taylor's expansion of $\mathcal{L}(\theta_{\parallel}^{(t+1)}, \theta_{\perp}^{(t)})$ around $\theta^{(t)}$ with Lipschitz smoothness Eq. (25), we have:

$$\mathcal{L}(\theta_{\parallel}^{(t+1)}, \theta_{\perp}^{(t)}) < \mathcal{L}(\theta_{\parallel}^{(t)}, \theta_{\perp}^{(t)}) + \nabla_{\theta_{\parallel}} \mathcal{L}(\theta^{(t)})^T (\theta_{\parallel}^{(t+1)} - \theta_{\parallel}^{(t)}) + \frac{c_u}{2} (\theta_{\parallel}^{(t+1)} - \theta_{\parallel}^{(t)})^T \sigma_{\parallel}^2 \mathbf{I}_D (\theta_{\parallel}^{(t+1)} - \theta_{\parallel}^{(t)})$$

1. **Logistic case:** From section A.4.1 Item 1 remember that the gradient step for logistic case is $\theta^{(t+1)} = \theta^{(t)} - \alpha \nabla_{\theta} \mathcal{L}(\theta^{(t)})$ with step size $\alpha \leq \frac{1}{c_u \sigma_{\parallel}^2}$ Eq. (42). Hence, $\theta_{\parallel}^{(t+1)} = \theta_{\parallel}^{(t)} - \alpha \nabla_{\theta_{\parallel}} \mathcal{L}(\theta^{(t)})$.

$$\Delta_{\parallel} \mathcal{L}(t) < -\alpha \|\nabla_{\theta_{\parallel}} \mathcal{L}(\theta^{(t)})\|^2 + \alpha^2 \frac{c_u \cdot \sigma_{\parallel}^2}{2} \|\nabla_{\theta_{\parallel}} \mathcal{L}(\theta^{(t)})\|^2$$

As $\alpha \leq \frac{1}{c_u \sigma_{\parallel}^2}$

$$\Delta_{\parallel} \mathcal{L}(t) < -(2c_u \sigma_{\parallel}^2)^{-1} \|\nabla_{\theta_{\parallel}} \mathcal{L}(\theta^{(t)})\|^2$$

2. **w-step:** From section A.4.1 Item 2 remember that the gradient step induced in the identifiable parameter θ , for w -step is $\theta^{(t+1)} = \theta^{(t)} - \alpha_1 \mathbf{A}^{(t/2)T} \mathbf{A}^{(t/2)} \nabla_{\theta} \mathcal{L}(\theta^{(t)})$ with step size $\alpha_1 \leq (M \cdot c_u \sigma_{\parallel}^2)^{-1}$ Eq. (43). Due to orthogonalization of the first layer, $\mathbf{A}^{(t/2)T} \mathbf{A}^{(t/2)} = \mathbf{I}_D$ and $\hat{\lambda}_{\mathbf{A}}, \check{\lambda}_{\mathbf{A}} = 1$ with $M = 1$. Hence, $\theta_{\parallel}^{(t+1)} = \theta_{\parallel}^{(t)} - \alpha_1 \nabla_{\theta_{\parallel}} \mathcal{L}(\theta^{(t)})$ and $\alpha_1 \leq (c_u \sigma_{\parallel}^2)^{-1}$. Now, mimicking the steps in the logistic case, we have:

$$\Delta_{\parallel} \mathcal{L}(t) < -(2c_u \sigma_{\parallel}^2)^{-1} \|\nabla_{\theta_{\parallel}} \mathcal{L}(\theta^{(t)})\|^2$$

3. **A-Step** From section A.4.1 Item 3 remember that the gradient step induced in the identifiable parameter θ , for **A**-step is $\theta^{(t+1)} = \theta^{(t)} - \alpha_2 \|w^{(t+1/2)}\|^4 \nabla_{\theta} \mathcal{L}(\theta^{(t)})$ with step size $\alpha_2 = (W \cdot c_u \sigma_{\parallel}^2)^{-1}$ Eq. (44). Hence, $\theta_{\parallel}^{(t+1)} = \theta_{\parallel}^{(t)} - \alpha_2 \|w^{(t+1/2)}\|^4 \nabla_{\theta_{\parallel}} \mathcal{L}(\theta^{(t)})$. Now, following identical the steps as in the logistic case, w -step, we have:

$$\Delta_{\parallel} \mathcal{L}(t) < -\|w^{(t+1/2)}\|^4 \cdot (2 \cdot W c_u \sigma_{\parallel}^2)^{-1} \|\nabla_{\theta} \mathcal{L}(\theta^{(t)})\|^2$$

A.4.3 Loss change off-manifold directions

$\Delta_{\perp} \mathcal{L}(t) = \mathcal{L}(\theta_{\parallel}^{(t)}, \theta_{\perp}^{(t+1)}) - \mathcal{L}(\theta^{(t)})$. Using Taylor's expansion of $\mathcal{L}(\theta_{\parallel}^{(t)}, \theta_{\perp}^{(t+1)})$ around $\theta^{(t)}$ with Lipschitz smoothness Eq. (24), we have:

$$\mathcal{L}(\theta_{\parallel}^{(t)}, \theta_{\perp}^{(t+1)}) < \mathcal{L}(\theta_{\parallel}^{(t)}, \theta_{\perp}^{(t)}) + \nabla_{\theta_{\perp}} \mathcal{L}(\theta^{(t)})^T (\theta_{\perp}^{(t+1)} - \theta_{\perp}^{(t)}) + \frac{c_u}{2} (\theta_{\perp}^{(t+1)} - \theta_{\perp}^{(t)})^T \sigma_{\perp}^2 \mathbf{I}_D (\theta_{\perp}^{(t+1)} - \theta_{\perp}^{(t)})$$

As $\sigma_{\perp} < \sigma_{\parallel}$, we have:

$$\mathcal{L}(\theta_{\parallel}^{(t)}, \theta_{\perp}^{(t+1)}) < \mathcal{L}(\theta_{\parallel}^{(t)}, \theta_{\perp}^{(t)}) + \nabla_{\theta_{\perp}} \mathcal{L}(\theta^{(t)})^T (\theta_{\perp}^{(t+1)} - \theta_{\perp}^{(t)}) + \frac{c_u}{2} (\theta_{\perp}^{(t+1)} - \theta_{\perp}^{(t)})^T \sigma_{\parallel}^2 \mathbf{I}_D (\theta_{\perp}^{(t+1)} - \theta_{\perp}^{(t)})$$

Follow identical steps corresponding to off-manifold direction as in section A.4.2 to get:

$$\begin{aligned} (\text{logistic step}) \quad \Delta_{\parallel} \mathcal{L}(t) &< -(2c_u \sigma_{\parallel}^2)^{-1} \|\nabla_{\theta_{\parallel}} \mathcal{L}(\theta^{(t)})\|^2 \\ (\text{w-step}) \quad \Delta_{\parallel} \mathcal{L}(t) &< -(2c_u \sigma_{\parallel}^2)^{-1} \|\nabla_{\theta_{\parallel}} \mathcal{L}(\theta^{(t)})\|^2 \\ (\text{A-step}) \quad \Delta_{\parallel} \mathcal{L}(t) &< -\|w^{(t+1/2)}\|^4 \cdot (2 \cdot W c_u \sigma_{\parallel}^2)^{-1} \|\nabla_{\theta} \mathcal{L}(\theta^{(t)})\|^2 \end{aligned}$$

□

Lemma A.4.1. Let $\theta^* = (\theta_{\parallel}^*, \theta_{\perp}^*)$ be the optimal identifiable parameter minimizing $\mathcal{L}(\gamma)$ and $\theta^{(t)}$ be the t^{th} iterate of θ induced by the optimization in logistic regression (Section 3.3.1) and 2-Linear Layer network setup (Section 3.3.2), then for $t_2 > t_1$ and appropriate $\alpha, \alpha_1, \alpha_2 \preceq \sigma_{\parallel}^{-2}$ we have:

$$\mathcal{L}(\theta_{\parallel}, \theta_{\perp}^{(t_2)}) \leq \mathcal{L}(\theta_{\parallel}, \theta_{\perp}^{(t_1)}); \forall \theta_{\parallel} \quad (45)$$

$$\mathcal{L}(\theta_{\parallel}^{(t_2)}, \theta_{\perp}) \leq \mathcal{L}(\theta_{\parallel}^{(t_1)}, \theta_{\perp}); \forall \theta_{\perp} \quad (46)$$

In particular, we have component-wise progressive bounds as such:

$$\mathcal{L}(\theta_{\parallel}, \theta_{\perp}^{(t+1)}) - \mathcal{L}(\theta_{\parallel}, \theta_{\perp}^{(t)}) \leq c_p (2c_u \sigma_{\perp}^2)^{-1} \|\nabla_{\theta_{\perp}} \mathcal{L}(\theta^{(t)})\|^2 \quad (47)$$

$$\mathcal{L}(\theta_{\parallel}^{(t+1)}, \theta_{\perp}) - \mathcal{L}(\theta_{\parallel}^{(t)}, \theta_{\perp}) \leq c_p (2c_u \sigma_{\parallel}^2)^{-1} \|\nabla_{\theta_{\parallel}} \mathcal{L}(\theta^{(t)})\|^2 \quad (48)$$

Proof. We will prove for the \perp direction; one can identically derive the result for the \parallel direction. Suppose we do T iteration of optimization; this induces a sequence in off-manifold parameters θ_\perp . $\theta_\perp^{(0)} \rightarrow \theta_\perp^{(1)} \rightarrow \dots \rightarrow \theta_\perp^{(T)}$. Fixing the \parallel parameter to general θ_\parallel , apply Taylor expansion with Lipschitz smoothness (lemma A.2.1) to the loss $\mathcal{L}(\theta_\parallel, \theta_\perp^{(t+1)})$ around the point $(\theta_\parallel, \theta_\perp^{(t)})$:

$$\mathcal{L}(\theta_\parallel, \theta_\perp^{(t+1)}) \leq \mathcal{L}(\theta_\parallel, \theta_\perp^{(t)}) + \nabla_{\theta_\perp} \mathcal{L}(\theta_\parallel, \theta_\perp^{(t)})^T (\theta_\perp^{(t+1)} - \theta_\perp^{(t)}) + \frac{c_u \sigma_\perp^2}{2} \|\theta_\perp^{(t+1)} - \theta_\perp^{(t)}\|^2$$

$\theta_\perp^{(t+1)} - \theta_\perp^{(t)} = -\check{\alpha} \nabla_{\theta_\perp} \mathcal{L}(\theta^{(t)})$ (Eq. (53)) for some step-size $\check{\alpha}$ depending on the situation.

$$\begin{aligned} \mathcal{L}(\theta_\parallel, \theta_\perp^{(t+1)}) &\leq \mathcal{L}(\theta_\parallel, \theta_\perp^{(t)}) - \check{\alpha} \nabla_{\theta_\perp} \mathcal{L}(\theta_\parallel, \theta_\perp^{(t)})^T \nabla_{\theta_\perp} \mathcal{L}(\theta^{(t)}) + \check{\alpha}^2 \frac{c_u \sigma_\perp^2}{2} \|\nabla_{\theta_\perp} \mathcal{L}(\theta^{(t)})\|^2 \\ &\stackrel{(i)}{\leq} \mathcal{L}(\theta_\parallel, \theta_\perp^{(t)}) - \check{\alpha} \cdot c \|\nabla_{\theta_\perp} \mathcal{L}(\theta^{(t)})\|^2 + \check{\alpha}^2 \frac{c_u \sigma_\perp^2}{2} \|\nabla_{\theta_\perp} \mathcal{L}(\theta^{(t)})\|^2 \\ &\leq \mathcal{L}(\theta_\parallel, \theta_\perp^{(t)}) - \check{\alpha} \underbrace{\|\nabla_{\theta_\perp} \mathcal{L}(\theta^{(t)})\|^2 \left(c - \check{\alpha} \frac{c_u \sigma_\perp^2}{2} \right)}_{\stackrel{(ii)}{\geq 0}} \\ &\leq \mathcal{L}(\theta_\parallel, \theta_\perp^{(t)}) - c_p (2c_u \sigma_\parallel^2)^{-1} \|\nabla_{\theta_\perp} \mathcal{L}(\theta^{(t)})\|^2 \end{aligned}$$

$c_p = c$ when $c \geq 1$ and $c_p = 2c - 1$ when $c < 1$.

(i) : $\nabla_{\theta_\perp} \mathcal{L}(\theta_\parallel, \theta_\perp^{(t)}) = -\mathbb{E}_{\sim x, y} y x_\perp \sigma(-y \cdot z) = -\mathbb{E}_{\sim x, y} y x_\perp (1 + \exp(y \theta_\parallel^T x_\parallel) \cdot \exp(y \theta_\perp^{(t)T} x_\perp))^{-1}$ Let $r = \exp(y \theta_\parallel^T x_\parallel) \cdot \exp(-y \theta_\perp^{(t)T} x_\perp)$. Then $\nabla_{\theta_\perp} \mathcal{L}(\theta_\parallel, \theta_\perp^{(t)}) = -\mathbb{E}_{\sim x, y} y x_\perp (1 + r \exp(y \theta_\parallel^{(t)T} x_\parallel) \cdot \exp(y \theta_\perp^{(t)T} x_\perp))^{-1} \stackrel{\text{As } r > 0}{=} -c \cdot \mathbb{E}_{\sim x, y} y x_\perp (1 + \exp(y \theta_\parallel^{(t)T} x_\parallel) \cdot \exp(y \theta_\perp^{(t)T} x_\perp))^{-1} = c \cdot \nabla_{\theta_\perp} \mathcal{L}(\theta^{(t)})$ for some $c > 0$.

(ii) : If $c \geq 1$ with $\check{\alpha} \leq (c_u \sigma_\parallel^2)^{-1}$ Eq. (54), then (ii) > 0 . If $0 < c < 1$, one can choose a strictly smaller step size still satisfying the upper bound of Eq. (54) $\check{\alpha} \leq c \cdot (c_u \sigma_\parallel^2)^{-1} < (c_u \sigma_\parallel^2)^{-1}$ which makes (ii) > 0 . As $\mathcal{L}(\theta_\parallel, \theta_\perp^{(t+1)}) \leq \mathcal{L}(\theta_\parallel, \theta_\perp^{(t)})$, for all t using induction $\mathcal{L}(\theta_\parallel, \theta_\perp^{(t_2)}) \leq \mathcal{L}(\theta_\parallel, \theta_\perp^{(t_1)})$ when $t_2 > t_1$. One can identically show that $\mathcal{L}(\theta_\parallel^{(t_2)}, \theta_\perp) \leq \mathcal{L}(\theta_\parallel^{(t_1)}, \theta_\perp)$. \square

A.5 Convergence Theorems

Proof of Theorem 4.2. We start with the proof of \perp direction; one can derive the result for \parallel mimicking similar steps with minor alteration. $\theta^* = (\theta_\parallel^*, \theta_\perp^*)$ is the optimal identifiable parameter value which minimizes the loss and takes T iteration of optimization.

Upper bound the Gradient norm by Loss difference: Using lemma A.4.1 with $t_2 = T, t_1 = t + 1$:

$$\mathcal{L}(\theta_\parallel^{(t)}, \theta_\perp^*) \leq \mathcal{L}(\theta_\parallel^{(t)}, \theta_\perp^{(t+1)})$$

Using lipschitz smoothness in \perp direction we have

$$\leq \mathcal{L}(\theta_\parallel^{(t)}, \theta_\perp^{(t)}) + \nabla_{\theta_\perp} \mathcal{L}(\theta^{(t)})^T (\theta_\perp^{(t+1)} - \theta_\perp^{(t)}) + \frac{c_u \sigma_\perp^2}{2} \|\theta_\perp^{(t+1)} - \theta_\perp^{(t)}\|^2$$

Gradient descent steps induce updates in \perp of the form, $\theta_\perp^{(t+1)} - \theta_\perp^{(t)} = -\check{\alpha} \nabla_{\theta_\perp} \mathcal{L}(\theta^{(t)})$

$$\leq \mathcal{L}(\theta_\parallel^{(t)}, \theta_\perp^{(t)}) - \check{\alpha} \|\nabla_{\theta_\perp} \mathcal{L}(\theta^{(t)})\|^2 \left(1 - \check{\alpha} \frac{c_u \sigma_\perp^2}{2} \right)$$

$$\implies \|\nabla_{\theta_\perp} \mathcal{L}(\theta^{(t)})\|^2 \leq \left(\mathcal{L}(\theta^{(t)}) - \mathcal{L}(\theta_\parallel^{(t)}, \theta_\perp^*) \right) \left(1 - \check{\alpha} \frac{c_u \sigma_\perp^2}{2} \right)^{-1} \cdot \check{\alpha}^{-1} \quad (49)$$

Similarly, for the on-manifold direction

$$\implies \|\nabla_{\theta_{\parallel}} \mathcal{L}(\theta^{(t)})\|^2 \leq \left(\mathcal{L}(\theta^{(t)}) - \mathcal{L}(\theta_{\parallel}^*, \theta_{\perp}^{(t)}) \right) \left(1 - \alpha_{\parallel} \frac{c_u \sigma_{\parallel}^2}{2} \right)^{-1} \cdot \check{\alpha}^{-1} \quad (50)$$

Also, using strong convexity Eq. (24) we have:

$$\begin{aligned} \mathcal{L}(\theta_{\parallel}^{(t)}, \theta_{\perp}^*) &\geq \mathcal{L}(\theta^{(t)}) + \nabla_{\theta_{\perp}} \mathcal{L}(\theta^{(t)})^T (\theta_{\perp}^* - \theta_{\perp}^{(t)}) + \frac{c_l \sigma_{\perp}^2}{2} \|\theta_{\perp}^* - \theta_{\perp}^{(t)}\|^2 \\ \nabla_{\theta_{\perp}} \mathcal{L}(\theta^{(t)})^T (\theta_{\perp}^* - \theta_{\perp}^{(t)}) &\geq \mathcal{L}(\theta^{(t)}) - \mathcal{L}(\theta_{\parallel}^{(t)}, \theta_{\perp}^*) + \frac{c_l \sigma_{\perp}^2}{2} \|\theta_{\perp}^* - \theta_{\perp}^{(t)}\|^2 \end{aligned} \quad (51)$$

Similarly, for the on-manifold direction, strong convexity leads to:

$$\nabla_{\theta_{\parallel}} \mathcal{L}(\theta^{(t)})^T (\theta_{\parallel}^{(t)} - \theta_{\parallel}^*) \geq \mathcal{L}(\theta^{(t)}) - \mathcal{L}(\theta_{\parallel}^*, \theta_{\perp}^{(t)}) + \frac{c_l \sigma_{\parallel}^2}{2} \|\theta_{\parallel}^* - \theta_{\parallel}^{(t)}\|^2 \quad (52)$$

Also, from Eq. (42), Eq. (43), Eq. (44)

$$\check{\alpha} = \begin{cases} \alpha & , \alpha \leq (c_u \sigma_{\parallel}^2)^{-1} \text{ (logistic)} \\ \alpha_1 & , \alpha_1 \leq (c_u \sigma_{\parallel}^2)^{-1} \text{ (w-step)} \\ \alpha_2 \|w^{(t+1/2)}\|^4 & , \alpha_2 \leq (W \cdot c_u \sigma_{\parallel}^2)^{-1}, \|w^{(t+1/2)}\|^4 < W, \forall t \text{ (A-step)} \end{cases} \quad (53)$$

$$\check{\alpha} \leq (c_u \sigma_{\parallel}^2)^{-1} \quad (54)$$

The parameter difference can be expressed in terms of the difference at the previous iteration:

$$\begin{aligned} \|\theta_{\perp}^{(t+1)} - \theta_{\perp}^*\|^2 &= \|\theta_{\perp}^{(t)} - \check{\alpha} \nabla_{\theta_{\perp}} \mathcal{L}(\theta^{(t)}) - \theta_{\perp}^*\|^2 \\ &= \|\theta_{\perp}^{(t)} - \theta_{\perp}^*\|^2 - 2\check{\alpha} \nabla_{\theta_{\perp}} \mathcal{L}(\theta^{(t)})^T (\theta_{\perp}^{(t)} - \theta_{\perp}^*) + \check{\alpha}^2 \|\nabla_{\theta_{\perp}} \mathcal{L}(\theta^{(t)})\|^2 \end{aligned}$$

Substituting Eq. (51)

$$\leq \|\theta_{\perp}^{(t)} - \theta_{\perp}^*\|^2 - 2\check{\alpha} \left(\mathcal{L}(\theta^{(t)}) - \mathcal{L}(\theta_{\parallel}^{(t)}, \theta_{\perp}^*) + \frac{c_l \sigma_{\perp}^2}{2} \|\theta_{\perp}^{(t)} - \theta_{\perp}^*\|^2 \right) + \check{\alpha}^2 \|\nabla_{\theta_{\perp}} \mathcal{L}(\theta^{(t)})\|^2$$

Using Eq. (49)

$$\begin{aligned} &\leq \|\theta_{\perp}^{(t)} - \theta_{\perp}^*\|^2 - 2\check{\alpha} \left(\mathcal{L}(\theta^{(t)}) - \mathcal{L}(\theta_{\parallel}^{(t)}, \theta_{\perp}^*) + \frac{c_l \sigma_{\perp}^2}{2} \|\theta_{\perp}^{(t)} - \theta_{\perp}^*\|^2 \right) \\ &+ \left(\mathcal{L}(\theta^{(t)}) - \mathcal{L}(\theta_{\parallel}^{(t)}, \theta_{\perp}^*) \right) \left(1 - \check{\alpha} \frac{c_u \sigma_{\perp}^2}{2} \right)^{-1} \cdot \check{\alpha} \end{aligned}$$

Using Eq. (54) and $\sigma_{\perp}/\sigma_{\parallel} < 1$

$$= \|\theta_{\perp}^{(t)} - \theta_{\perp}^*\|^2 (1 - \check{\alpha} c_l \sigma_{\perp}^2) + \underbrace{\left(\mathcal{L}(\theta_{\perp}^{(t)}, \theta_{\parallel}) - \mathcal{L}(\theta_{\perp}^*, \theta_{\parallel}) \right)}_{\leq 0} \cdot \underbrace{\left((1 - \check{\alpha} \frac{c_u \sigma_{\perp}^2}{2})^{-1} - 2 \right)}_{\leq 2} \cdot \check{\alpha}$$

Using Eq. (54) and $c_l < c_u$ Eq. (23).

$$\leq \|\theta_{\perp}^{(t)} - \theta_{\perp}^*\|^2 \underbrace{\left(1 - \frac{c_l \sigma_{\perp}^2}{c_u \sigma_{\parallel}^2} \right)}_{\leq 1}$$

Suppose we have T total iterations then, inductively the equations accumulate over as:

$$\|\theta_{\perp}^{(T)} - \theta_{\perp}^*\|^2 \leq \|\theta_{\perp}^{(0)} - \theta_{\perp}^*\|^2 \left(1 - \frac{c_l \sigma_{\perp}^2}{c_u \sigma_{\parallel}^2} \right)^T \leq \|\theta_{\perp}^{(0)} - \theta_{\perp}^*\|^2 \exp \left(-T \frac{c_l \sigma_{\perp}^2}{c_u \sigma_{\parallel}^2} \right) \quad (55)$$

Hence, we require $T \geq \frac{c_u \sigma_{\parallel}^2}{c_l \sigma_{\perp}^2} \log \left(\frac{\|\theta_{\perp}^{(0)} - \theta_{\perp}^*\|}{\delta} \right)$ for $\mathcal{O}(\delta)$ distance from θ_{\perp}^* .

Similarly, one can derive the bound for the \parallel direction mimicking the exact steps as \perp direction but instead using analogous equations Eq. (52), Eq. (50).

$T \geq \frac{c_u \sigma_{\parallel}^2}{c_u \sigma_{\parallel}^2} \log \left(\frac{\|\theta_{\parallel}^{(0)} - \theta_{\parallel}^*\|}{\delta} \right) = \log \left(\frac{\|\theta_{\parallel}^{(0)} - \theta_{\parallel}^*\|}{\delta} \right)$ for $\mathcal{O}(\delta)$ distance from θ_{\parallel}^* .

Remark A.1. When deriving the bounds for $\|\theta_{\parallel}^{(0)} - \theta_{\parallel}^*\|$ vs $\|\theta_{\perp}^{(0)} - \theta_{\perp}^*\|$, the key point of difference is using the same step size $\alpha \preceq \sigma_{\parallel}^{-2}$ even though the strong convexity constants are different, $\propto \sigma_{\parallel}^2$ for \parallel direction and $\propto \sigma_{\perp}^2$ for \perp direction. This introduces the ratio $\sigma_{\perp}/\sigma_{\parallel}$ in the \perp case, while for \parallel case the step size and strong-convexity parameter neutralize each other to 1. Hence, if we could enforce separate step size for \perp, \parallel directions $\alpha_{\perp} \preceq \sigma_{\perp}^{-2}, \alpha_{\parallel} \preceq \sigma_{\parallel}^{-2}$. Then, we can get equivalent rates in both directions.

□

Proof of Theorem 4.3. We want to minimize the loss $\mathcal{L}(\theta) = \mathbb{E}_{\sim x, y} \ell(y \cdot z)$. The minimum loss that can be attained has a natural lower bound $\min_{\theta} \mathcal{L}(\theta) \geq (1 - \nu) \cdot \min_{\theta} \mathbb{E}_{\sim x, y | \emptyset} \ell(y \cdot z) + \nu \min_{\theta} \mathbb{E}_{\sim x, y | \neg \emptyset} \ell(y \cdot z)$. Suppose we only optimize the loss w.r.t. θ_{\parallel} and $\theta_{\perp} = \mathbf{0}$, then a perfect classifier on \parallel direction can distinguish x_{\parallel} with probability 1 or 0 loss, but only with $1/2$ probability on \perp direction. In this case, $\min_{\theta_{\parallel}} \mathcal{L}(\theta) \geq \nu \log 2$. In general, the classifier isn't perfect, and θ_{\perp} can be fixed at some default value. Hence, the lower bound is controlled by $\nu \log 2$ up to a constant $\min_{\theta_{\parallel}} \mathcal{L}(\theta) \geq C = \Omega(\nu \log 2)$. Consider two cases when the loss tolerance $\delta < C$ or $> C$.

Case 1: $\delta < C$

From the progressive bounds in proof of Theorem 4.1 for any optimization iterate (logistic, w-step or A-step) induced in the identifiable parameter θ , has a decremental loss:

$$\mathcal{L}(\theta^{(t+1)}) - \mathcal{L}(\theta^{(t)}) \leq -(2c_u \sigma_{\parallel}^2)^{-1} \|\nabla_{\theta} \mathcal{L}(\theta^{(t)})\|^2 \quad (56)$$

$$-2c_l \sigma_{\perp}^2 \cdot (\mathcal{L}(\theta^{(t)}) - \mathcal{L}(\theta^*)) \geq -\|\nabla_{\theta} \mathcal{L}(\theta^{(t)})\|^2 \quad (\text{PL-inequality})$$

Proof of PL inequality: The Eq. (PL-inequality) is a consequence of strong convexity. Using strong convexity in the space of identifiable parameter θ Lemma A.2.1, Eq. (23) we have:

$$\mathcal{L}(\theta) \geq \mathcal{L}(\theta^{(t)}) + \nabla_{\theta} \mathcal{L}(\theta^{(t)})^T (\theta - \theta^{(t)}) + \frac{c_l}{2} (\theta - \theta^{(t)})^T \begin{pmatrix} \sigma_{\parallel}^2 \mathbf{I}_d & \mathbf{0} \\ \mathbf{0} & \sigma_{\perp}^2 \mathbf{I}_g \end{pmatrix} (\theta - \theta^{(t)})$$

$$\mathcal{L}(\theta) \geq \mathcal{L}(\theta^{(t)}) + \nabla_{\theta} \mathcal{L}(\theta^{(t)})^T (\theta - \theta^{(t)}) + \frac{c_l \cdot \sigma_{\perp}^2}{2} \|\theta - \theta^{(t)}\|^2$$

Minimizing both sides w.r.t θ , happens for $\theta = \theta^{(t)} - \nabla_{\theta} \mathcal{L}(\theta^{(t)}) (c_l \sigma_{\perp}^2)^{-1}$

$$\mathcal{L}(\theta^*) \geq \mathcal{L}(\theta^{(t)}) - \|\nabla_{\theta} \mathcal{L}(\theta^{(t)})\|^2 (2c_l \sigma_{\perp}^2)^{-1} \quad \square$$

Hence, from the progressive bound, we have Eq. (56) :

$$\mathcal{L}(\theta^{(t+1)}) \leq \mathcal{L}(\theta^{(t)}) - (2c_u \sigma_{\parallel}^2)^{-1} \|\nabla_{\theta} \mathcal{L}(\theta^{(t)})\|^2$$

Subtracting $\mathcal{L}(\theta^*)$ from both sides

$$\mathcal{L}(\theta^{(t+1)}) - \mathcal{L}(\theta^*) \leq \mathcal{L}(\theta^{(t)}) - \mathcal{L}(\theta^*) - (2c_u \sigma_{\parallel}^2)^{-1} \|\nabla_{\theta} \mathcal{L}(\theta^{(t)})\|^2$$

Using Eq. (PL-inequality)

$$\mathcal{L}(\theta^{(t+1)}) - \mathcal{L}(\theta^*) \leq (\mathcal{L}(\theta^{(t)}) - \mathcal{L}(\theta^*)) \cdot \left(1 - \frac{c_l \sigma_{\perp}^2}{c_u \sigma_{\parallel}^2} \right)$$

Suppose we have T total iterations; then, inductively, the equations accumulate over as:

$$\mathcal{L}(\theta^{(T)}) - \mathcal{L}(\theta^*) \leq \left(\mathcal{L}(\theta^{(0)}) - \mathcal{L}(\theta^*) \right) \left(1 - \frac{c_l \sigma_{\perp}^2}{c_u \sigma_{\parallel}^2} \right)^T \leq \left(\mathcal{L}(\theta^{(0)}) - \mathcal{L}(\theta^*) \right) \exp \left(-T \frac{c_l \sigma_{\perp}^2}{c_u \sigma_{\parallel}^2} \right) \quad (57)$$

Hence, we require $T \geq \frac{c_u \sigma_{\parallel}^2}{c_l \sigma_{\perp}^2} \log((\mathcal{L}(\theta^{(0)}) - \mathcal{L}(\theta^*)) \delta^{-1})$ for $\mathcal{O}(\delta)$ error tolerance. This is rate r_2 in the thm statement.

Case 2: $\delta > C$

The rate r_2 proved in the previous case is universal and holds for this case as well. However, we can obtain a better rate in this scenario.

In this case, the loss can attain value δ solely by optimizing θ_{\parallel} . Therefore, we will upper bound the original gradient descent loss sequence by a loss sequence solely dependant on updates of θ_{\parallel} , and we will see that because convergence is better on θ_{\parallel} direction, we can get better rates.

Note that if $\mathcal{L}(\theta) = C$, then using Jensen's inequality for convex functions: $\ell(\mathbb{E}_{\sim x, y} y \cdot z) \leq \mathcal{L}(\theta) = C$.

$$\begin{aligned} \ln(1 + \exp(-\mathbb{E} y \theta^T x)) &\leq C \\ \exp(-\mathbb{E} y \theta^T x) &\leq e^C - 1 \\ \mathbb{E} y \theta^T x &\geq \ln\left(\frac{1}{e^C - 1}\right) \\ \mathbb{E} y(\langle \theta_{\parallel}, x_{\parallel} \rangle + \langle \theta_{\perp}, x_{\perp} \rangle) &\geq \ln\left(\frac{1}{e^C - 1}\right) \\ \pi(\langle \theta_{\parallel}, \mu_{\parallel}^{(1)} \rangle + \langle \theta_{\perp}, \mu_{\perp}^{(1)} \rangle) - (1 - \pi)(\langle \theta_{\parallel}, \mu_{\parallel}^{(-1)} \rangle + \langle \theta_{\perp}, \mu_{\perp}^{(-1)} \rangle) &\geq \ln\left(\frac{1}{e^C - 1}\right) \end{aligned}$$

Note that the above can always be satisfied by $\theta_{\parallel} = c' \cdot \mu_{\parallel}^{(1)} - c'' \cdot \mu_{\parallel}^{(-1)}$ for appropriate choice of constants c', c'' . Hence for a fixed θ_{\perp} there always exists some $\tilde{\theta}_{\parallel}$ such that $\mathcal{L}(\tilde{\theta}_{\parallel}, \theta_{\perp}) < C \implies \mathcal{L}(\tilde{\theta}_{\parallel}, \theta_{\perp}) - \mathcal{L}(\theta^*) < C$. This means fixing $\theta_{\perp} = \theta_{\perp}^{(0)}$ at initialization, there exists $\tilde{\theta}_{\parallel}$ as well which satisfies:

$$\min_{\theta_{\parallel}} \mathcal{L}(\theta_{\parallel}, \theta_{\perp}^{(0)}) - \mathcal{L}(\theta^*) \leq \mathcal{L}(\tilde{\theta}_{\parallel}, \theta_{\perp}^{(0)}) - \mathcal{L}(\theta^*) < C \quad (58)$$

Using lemma A.4.1 we have:

$$\mathcal{L}(\theta^{(T)}) \leq \mathcal{L}(\theta_{\parallel}^{(T)}, \theta_{\perp}^{(0)})$$

Subtracting $\mathcal{L}(\theta^*)$ both sides

$$\begin{aligned} \mathcal{L}(\theta^{(T)}) - \mathcal{L}(\theta^*) &\leq \mathcal{L}(\theta_{\parallel}^{(T)}, \theta_{\perp}^{(0)}) - \mathcal{L}(\theta^*) \\ &= \mathcal{L}(\theta_{\parallel}^{(T)}, \theta_{\perp}^{(0)}) - \min_{\theta_{\parallel}} \mathcal{L}(\theta_{\parallel}, \theta_{\perp}^{(0)}) + \min_{\theta_{\parallel}} \mathcal{L}(\theta_{\parallel}, \theta_{\perp}^{(0)}) - \mathcal{L}(\theta^*) \\ &\leq (\delta - C) + C = \delta \end{aligned} \quad (59)$$

Hence, if we find a T for which $\mathcal{L}(\theta_{\parallel}^{(T)}, \theta_{\perp}^{(0)}) - \min_{\theta_{\parallel}} \mathcal{L}(\theta_{\parallel}, \theta_{\perp}^{(0)}) \leq \delta - C$ then we are done.

From lemma A.4.1, Eq. (48) we have a progressive bound on the off-manifold component as follows:

$$\begin{aligned} \mathcal{L}(\theta_{\parallel}^{(t+1)}, \theta_{\perp}^{(0)}) &\leq \mathcal{L}(\theta_{\parallel}^{(t)}, \theta_{\perp}^{(0)}) - c_p (2c_u \sigma_{\parallel}^2)^{-1} \|\nabla_{\theta_{\parallel}} \mathcal{L}(\theta^{(t)})\|^2 \\ -2c'_p c_l \sigma_{\parallel}^2 \cdot \left(\mathcal{L}(\theta_{\parallel}^{(t)}, \theta_{\perp}^{(0)}) - \min_{\theta_{\parallel}} \mathcal{L}(\theta_{\parallel}, \theta_{\perp}^{(0)}) \right) &\geq -\|\nabla_{\theta_{\parallel}} \mathcal{L}(\theta^{(t)})\|^2 \end{aligned} \quad (60)$$

Proof of PL inequality: The Eq. (PL-inequality) is a consequence of strong convexity. Using strong convexity w.r.t. θ_{\parallel} Lemma A.2.1, Eq. (25) we have:

$$\mathcal{L}(\theta_{\parallel}, \theta_{\perp}^{(0)}) \geq \mathcal{L}(\theta_{\parallel}^{(t)}, \theta_{\perp}^{(0)}) + \nabla_{\theta_{\parallel}} \mathcal{L}(\theta_{\parallel}^{(t)}, \theta_{\perp}^{(0)})^T (\theta_{\parallel} - \theta_{\parallel}^{(t)}) + \frac{c_l \cdot \sigma_{\parallel}^2}{2} \|\theta_{\parallel} - \theta_{\parallel}^{(t)}\|^2$$

Minimizing both sides w.r.t $\theta_{||}$, happens for $\theta_{||} = \theta_{||}^{(t)} - \nabla_{\theta_{||}} \mathcal{L}(\theta_{||}^{(t)}, \theta_{\perp}^{(0)})(c_l \sigma_{||}^2)^{-1}$

$$\min_{\theta_{||}} \mathcal{L}(\theta_{||}, \theta_{\perp}^{(0)}) \geq \mathcal{L}(\theta_{||}^{(t)}, \theta_{\perp}^{(0)}) - \|\nabla_{\theta_{||}} \mathcal{L}(\theta_{||}^{(t)}, \theta_{\perp}^{(0)})\|^2 (2c_l \sigma_{||}^2)^{-1}$$

From arguments like (i) in proof of lemma A.4.1, we know $c'_p \|\nabla_{\theta_{||}} \mathcal{L}(\theta_{||}^{(t)}, \theta_{\perp}^{(0)})\|^2 = \|\nabla_{\theta_{||}} \mathcal{L}(\theta^{(t)})\|^2$ for some proportionality constant c'_p

$$\min_{\theta_{||}} \mathcal{L}(\theta_{||}, \theta_{\perp}^{(0)}) \geq \mathcal{L}(\theta_{||}^{(t)}, \theta_{\perp}^{(0)}) - \|\nabla_{\theta_{||}} \mathcal{L}(\theta^{(t)})\|^2 (2c'_p c_l \sigma_{||}^2)^{-1} \quad \square$$

Hence, from the progressive bound, we have Eq. (60) :

$$\mathcal{L}(\theta_{||}^{(t+1)}, \theta_{\perp}^{(0)}) \leq \mathcal{L}(\theta_{||}^{(t)}, \theta_{\perp}^{(0)}) - c_p (2c_u \sigma_{||}^2)^{-1} \|\nabla_{\theta_{||}} \mathcal{L}(\theta^{(t)})\|^2$$

Subtracting $\min_{\theta_{||}} \mathcal{L}(\theta_{||}, \theta_{\perp}^{(0)})$ from both sides

$$\mathcal{L}(\theta_{||}^{(t+1)}, \theta_{\perp}^{(0)}) - \min_{\theta_{||}} \mathcal{L}(\theta_{||}, \theta_{\perp}^{(0)}) \leq \mathcal{L}(\theta_{||}^{(t)}, \theta_{\perp}^{(0)}) - \min_{\theta_{||}} \mathcal{L}(\theta_{||}, \theta_{\perp}^{(0)}) - c_p (2c_u \sigma_{||}^2)^{-1} \|\nabla_{\theta_{||}} \mathcal{L}(\theta^{(t)})\|^2$$

Using Eq. (PL-inequality $\theta_{||}$)

$$\mathcal{L}(\theta_{||}^{(t+1)}, \theta_{\perp}^{(0)}) - \min_{\theta_{||}} \mathcal{L}(\theta_{||}, \theta_{\perp}^{(0)}) \leq \left(\mathcal{L}(\theta_{||}^{(t)}, \theta_{\perp}^{(0)}) - \min_{\theta_{||}} \mathcal{L}(\theta_{||}, \theta_{\perp}^{(0)}) \right) \cdot \left(1 - \frac{c_p c_l c'_p}{c_u} \right)$$

Suppose we have T total iterations; then, inductively, the equations accumulate over as:

$$\begin{aligned} \mathcal{L}(\theta_{||}^{(T)}, \theta_{\perp}^{(0)}) - \min_{\theta_{||}} \mathcal{L}(\theta_{||}, \theta_{\perp}^{(0)}) &\leq \left(\mathcal{L}(\theta^{(0)}) - \min_{\theta_{||}} \mathcal{L}(\theta_{||}, \theta_{\perp}^{(0)}) \right) \left(1 - \frac{c_p c_l c'_p}{c_u} \right)^T \\ &\leq \left(\mathcal{L}(\theta^{(0)}) - \min_{\theta_{||}} \mathcal{L}(\theta_{||}, \theta_{\perp}^{(0)}) \right) \exp \left(-T \frac{c_p c_l c'_p}{c_u} \right) \\ &\leq \left(\mathcal{L}(\theta^{(0)}) - \mathcal{L}(\theta^*) \right) \exp \left(-T \frac{c_p c_l c'_p}{c_u} \right) \end{aligned}$$

Hence, we require $T \geq \frac{c_u}{c_p c_l c'_p} \log \left((\mathcal{L}(\theta^{(0)}) - \mathcal{L}(\theta^*)) (\delta - C)^{-1} \right)$ for $\mathcal{L}(\theta_{||}^{(T)}, \theta_{\perp}^{(0)}) - \min_{\theta_{||}} \mathcal{L}(\theta_{||}, \theta_{\perp}^{(0)}) < \delta - C$. Hence, validating the series of equations Eq. (59) and implying $\mathcal{L}(\theta^{(T)}) - \mathcal{L}(\theta^*) \leq \delta$. This gives us the rate r_1 in theorem 4.3. Note that the rate r_2 holds regardless of δ value. The final rate is the minimum of the two rates. \square

B Additional Experimental Details

A learning rate of 10^{-3} with default ADAM parameters were used for clean training. For generating PGD attacks a step size of $\frac{2}{255}$ with $\lfloor \epsilon \cdot \frac{255}{2} \rfloor$ (ϵ is the attack strength) attack iterations and 1 restart was used. For KFAC preconditioner, the default hyper-parameters were used.

Compute resource: A single NVIDIA V100 gpu was used, requiring 2hrs, 3.5 hrs (MNIST, FMNIST 1000 epochs) per run for ADAM and ADAM+KFAC respectively. For CIFAR10 ADAM experiments it took 6 hrs per run (4000 epochs). Attack time included.

Layers
Conv2d(1, 16, 4, stride=2, padding=1), ReLU
Conv2d(16, 32, 4, stride=2, padding=1), ReLU
Linear(32*7*7, 100), ReLU
Linear(100, 10)

Table 1: NN architecture FMNIST/MNIST.

Layers
Conv2d(1, 16, 4, stride=2, padding=1), BatchNorm2d(16), ReLU
Conv2d(16, 32, 4, stride=2, padding=1), BatchNorm2d(32), ReLU
Linear(32*7*7,100), BatchNorm2d(100), ReLU
Linear(100, 10)

Table 2: NN architecture FMNIST/MNIST with BN.

Layers
Conv2d(3, 128, 5, padding=2), ReLU
Conv2d(128, 128, 5, padding=2), ReLU,
MaxPool2d(2,2), Conv2d(128, 256, 3, padding=1), ReLU,
Conv2d(256, 256, 3, padding=1), ReLU,
MaxPool2d(2,2), Flatten(), Linear(256*8*8,1024), ReLU,
Linear(1024, 512), ReLU
Linear(512, 10)

Table 3: NN architecture CIFAR10.

Layers
Conv2d(3, 128, 5, padding=2), ReLU
BatchNorm2d(128)
Conv2d(128, 128, 5, padding=2), ReLU,
BatchNorm2d(128),
MaxPool2d(2,2), Conv2d(128, 256, 3, padding=1), ReLU,
BatchNorm2d(256),
Conv2d(256, 256, 3, padding=1), ReLU,
BatchNorm2d(256),
MaxPool2d(2,2), Flatten(), Linear(256*8*8,1024), ReLU,
BatchNorm1d(1024)
Linear(1024, 512), ReLU
BatchNorm1d(512)
Linear(512, 10)

Table 4: NN architecture CIFAR10 with BN.